

Engineers, Proceedings
VOLUME 84 NO. HY7

DECEMBER 1958

PART 1

JOURNAL of the

***Hydraulics
Division***

UNIVERSITY OF HAWAII
LIBRARY
JAN 15 1959

PROCEEDINGS OF THE



**AMERICAN SOCIETY
OF CIVIL ENGINEERS**

CI
439

Journal of the
HYDRAULICS DIVISION
Proceedings of the American Society of Civil Engineers

HYDRAULICS DIVISION
EXECUTIVE COMMITTEE
Carl E. Kindsvater, Chairman; Arthur T. Ippen, Vice-Chairman; Harold M.
Martin; Maurice L. Dickinson; Joseph B. Tiffany, Jr., Secretary

COMMITTEE ON PUBLICATIONS
James W. Ball, Chairman; Haywood G. Dewey, Jr.; Eugene P. Fortson, Jr.;
Carl E. Kindsvater; Joseph B. Tiffany, Jr.

CONTENTS

December, 1958

Papers

	Number
Hydrological Aspects of Storm Surge Generation	
by D. Lee Harris	1859
Discussion	1880
Experiments on Self-Aerated Flow in Open Channels	
by Lorenz G. Straub and Alvin G. Anderson	1890

Journal of the
HYDRAULICS DIVISION

Proceedings of the American Society of Civil Engineers

METEOROLOGICAL ASPECTS OF STORM SURGE GENERATION^a

D. Lee Harris¹
(Proc. Paper 1859)

INTRODUCTION

The coastal floods, produced by Hurricane AUDREY in June 1957 claimed more than 300⁽¹⁾ lives and destroyed more than 100 homes. Even in this enlightened year of 1957, when hurricane warnings are broadcast by radio and television long before the storm arrives, the high tides produced by the storm continue to claim more lives than all other aspects of hurricane behavior. Although many of the newcomers in the Cameron area evacuated the threatened region soon after the hurricane warnings were announced, many of the old-timers remained because they had weathered previous hurricanes with little difficulty and they did not expect this one to be more severe than the others. Few facts concerning hurricanes and their effects on sea level, which if fully understood, may prevent future disasters of this kind, are presented in this paper.

This paper is concerned primarily with the meteorological aspects of storm surge generation by hurricanes. The physical aspects of hurricane storm surge behavior along the Atlantic and Gulf coasts of the United States have been discussed in greater detail in Harris.⁽²⁾ Zetler⁽³⁾ gave an extensive treatment of the effects of hurricanes on sea level at Charleston, S. C. Field and Miller⁽⁴⁾ considered the effects of several recent Atlantic Coast hurricanes. Hubert and Clark⁽⁵⁾ published charts showing the high water marks established after 16 Atlantic and Gulf coast hurricanes. Reid⁽⁶⁾ developed a storm tide index based on the size and intensity of the hurricane and slope of the continental shelf.

^a Discussion open until May 1, 1959. To extend the closing date one month, a written request must be filed with the Executive Secretary, ASCE. Paper 1859 is part of the copyrighted Journal of the Hydraulics Division, Proceedings of the American Society of Civil Engineers, Vol. 84, No. HY 7, December, 1958.

Presented at the ASCE Hydraulics Conference in Cambridge, Mass., August, 1957.

¹Office of Meteorological Research, Storm Surge Research Unit, U. S. Weather Bureau, Washington, D. C.

Hurricane Models

The wind and pressure distributions of a hurricane are never known with desired accuracy before the storm strikes land. Hence, in forecasting storm surges and in the design of engineering works to be constructed as protection from some future hurricane, it is necessary to use a storm model. Such models can be constructed in a variety of ways depending on the use for which they are intended. For storm surge work it is desired to describe as accurately as possible the distribution of atmospheric pressure and sustained wind speeds near the surface of the sea.

The pressure in many hurricanes can be represented with a close approximation by an equation of the type

$$P = P_o + (P_n - P_o) F(r/R),$$

where P_n = the pressure just outside the storm,

P_o = the pressure at the center of the storm,

R = some characteristic radius of the storm,

r = distance from the center of the storm,

$F(r/R)$ indicates a function of r/R .

The radius of the eye, the distance from the center to the zone of maximum winds, and the distance from the center to the outermost closed isobar have all been suggested for use as the characteristic radius. The proper choice probably depends on whether it is desired to obtain the maximum accuracy in the high wind speed zone or for the entire storm. $(P_n - P_o)$ is intended as a measure of the intensity of the storm, but P_n is likewise difficult to define explicitly. Some workers prefer to use the pressure of the outermost closed isobar, still others prefer some other definition. Virtually all workers in this field use the best obtainable estimate of the lowest pressure in the storm for P_o . Because an objective definition of P_o is easily constructed, many writers use this value to estimate the intensity of the storm.

The first approximation of the wind speed within any cyclone is given by the gradient wind equation. This can be expressed in terms similar to Eq. (1) by:

$$V_g^2/r + fV_g = \rho^{-1}(P_n - P_o) F'(r/R).$$

V_g = gradient wind speed

f = coriolis parameter

ρ = density of air

F' = derivative of F with respect to (r/R)

Near the center of a hurricane V_g^2/r is considerably larger than fV_g ; hence the second term on the left can be neglected within the accuracy of this approximation. Thus the gradient wind, and presumably, the true surface wind speed, is approximately proportional to the square root of $(P_n - P_o)$. This relationship is often used in estimating the maximum wind speed in a hurricane. (11)

A hurricane model developed along the lines indicated by Eqs. (1) and (2) is described by the following equations:

$$\frac{P - P_o}{P_n - P_o} = e^{-R/r} \quad (3)$$

$$v_g^2/r + f v_g = \frac{1}{f} (P_n - P_o) e^{-R/r} \quad (4)$$

The symbol R in this model has been identified with the radius of maximum wind speed. The agreement between this model and the observations of an exceptionally well observed hurricane is shown in Fig. 1. The insert map gives the storm track. The dots on the left give the observed pressure at several stations in the vicinity of Lake Okeechobee, Florida. The solid line gives the theoretical pressure profile fitted to three points within 50 miles of the storm center. The corresponding theoretical wind profile is given by the upper curve on the right hand side of the figure. The observed winds at one station are given by the dots below this curve. A solid line has been drawn through these dots by eye in order to obtain a smooth profile. The observed wind speed varies in a systematic way from about 65% of the computed wind speed at the outer edge of the data shown to almost 90% of the predicted value near the zone of maximum wind speed. Equally good agreement between the theoretical and observed wind speeds has been obtained in only a few storms. This lack of agreement between the theoretical and observed winds is due in part to the elementary nature of the model, but perhaps equally to the lack of first class wind records near the center of hurricanes. The parameters for this model have been computed for a large number of storms and were first published in Hydrometeorological Report No. 32.⁽⁷⁾

Data for new storms are added and data for old storms are corrected as new information becomes available. An up-to-date (August 1, 1957) version of these data is included in this paper in Table I.

Eqs. (2) and (4) can be valid only for stationary storms. The wind speeds on the right hand side of a moving storm are generally higher than those observed to the left of the storm track. A simple but incomplete explanation, widely accepted for more than half a century, is based on the assumption that the forward speed of the storm must be added to the rotary speed on the right hand side and subtracted on the left. This would give an asymmetry in the wind velocity on the right and left sides of the storm track due to the forward speed of the storm. This assumption usually leads to corrections in the right direction but not of the proper magnitude. Winds of hurricane intensity are significantly affected by friction with the underlying water or land surface. The effects of friction and of the inflow necessary to feed the vertical currents, prominent throughout the region of hurricane winds, may exceed the effects of the forward motion of the storm, at least near the surface.

Although Eq. (4) is too simple to permit an adequate determination of the wind field in a hurricane, it is possible to make use of empirically derived relations between the wind speed at nearby locations over water and over land, and between the observed wind speed over various types of frictional surfaces and the theoretical wind speed to determine a usefully accurate picture of the wind field. Figs. 2a and b show the reconstructed pressure and wind fields for the New England Hurricane of September 21, 1938.⁽⁸⁾ In the derivation of

DATE	P _o in.	P _n in.	P _n -P _o in.	P _o mb.	P _n mb.	P _n -P _o mb.
Aug. 28, 1893	28.28	29.61	1.33	958	1003	45
Oct. 1, 1893	28.22	29.99	1.77	956	1016	60
Oct. 13, 1893	28.33	29.61	1.28	959	1003	44
Oct. 2, 1898	28.82	30.03	1.21	976	1017	41
Oct. 31, 1899	28.70	30.49	1.79	972	1033	61
Sept. 8, 1900	27.64	29.78	2.14	936	1009	73
Aug. 14, 1901	28.72	30.16	1.44	973	1021	48
Sept. 11, 1903	28.84	30.12	1.28	977	1020	43
June 17, 1906	28.91	29.98	1.07	979	1015	36
Sept. 17, 1906	28.98	30.38	1.40	981	1029	48
Sept. 27, 1906	28.50	30.07	1.57	965	1018	53
Oct. 18, 1906	28.84	29.80	.96	977	1009	32
July 21, 1909	28.31	30.27	1.96	959	1025	66
Sept. 20, 1909	28.94	30.30	1.36	980	1026	46
Oct. 11, 1909	28.30	30.07	1.77	958	1018	60
Oct. 17, 1910	27.80	29.19	1.39	941	989	48
* Oct. 18, 1910	28.33	29.77	1.44	959	1008	49
Aug. 28, 1911	28.92	30.10	1.18	979	1019	40
Sept. 3, 1913	28.81	29.98	1.17	976	1015	39
Aug. 17, 1915	28.01	29.65	1.64	949	1004	55
Sept. 29, 1915	27.70	30.14	2.44	938	1021	83
July 5, 1916	28.38	30.03	1.65	961	1017	56
Aug. 18, 1916	28.00	30.77	2.77	948	1042	94
Oct. 18, 1916	28.76	30.20	1.44	974	1023	49
Sept. 28, 1917	28.48	29.88	1.40	964	1012	48
Sept. 9, 1919	27.44	29.73	2.29	929	1007	78
* Sept. 14, 1919	P _o near 28.0 inches					
Sept. 21, 1920	28.93	29.90	.97	980	1013	33
June 22, 1921	28.17	30.03	1.86	954	1017	63
Oct. 25, 1921	28.29	29.59	1.30	958	1002	44
Aug. 25, 1924	28.70	30.33	1.63	972	1027	55
* Aug. 26, 1924	28.70	29.62	.92	972	1003	31
Oct. 19, 1924	28.70	29.82	1.12	972	1010	38
* Oct. 20, 1924	28.83	29.62	.79	976	1003	27
Dec. 2, 1925	28.95	29.90	.95	980	1013	33
July 28, 1926	28.34	29.91	1.57	960	1013	53
Aug. 25, 1926	28.31	30.35	2.04	959	1028	69
Sept. 18, 1926	27.59	29.99	2.40	934	1016	82
* Sept. 20, 1926	28.20	30.13	1.93	955	1020	65
Oct. 20, 1926	27.52	29.97	2.45	932	1015	83
Sept. 16, 1928	27.62	30.38	2.76	935	1029	94
June 28, 1929	28.62	29.97	1.35	969	1015	46
Sept. 28, 1929	28.15	30.08	1.93	953	1019	66

Table I - Characteristics of United States Hurricanes

c kt	t _c hrs.	P _a		STATION	r _a n.mi.
		in.	mb.		
15	4	28.28	958	Savannah, Ga.	2
7	4	28.65	970	Moss Point, Miss.	13
21	4	28.33	959	South Island, S. C.	1
11	4	29.12	986	Jacksonville, Fla.	23
18	4	28.90	979	Charleston, S. C.	50
10	4	28.48	964	Galveston, Tex.	17
14	4	29.42(1)	996	New Orleans, La.	45
7	3	29.47	998	Tampa, Fla.	14
12	4	29.46	998	Jupiter, Fla.	29
16	4	29.50	999	Columbia, S. C.	28
16	4	28.50	965	Ship at Scranton, Miss.	5
6	4	29.26	991	Jupiter, Fla.	33
12	4	29.00	982	Bay City, Tex.	16
11	4	29.23	990	New Orleans, La.	43
10	4	28.36	960	Sand Key, Fla.	7
11	4	27.80	941	S.S.Jean Nr. Tortugas, Fla.	0
11	4	28.94	980	Tampa, Fla.	45
8	4	29.02	983	Savannah, Ga.	6
16	4	29.36	994	Raleigh, N. C.	6
11	4	28.14	953	Velasco, Tex.	11
10	4	28.01	949	New Orleans, La.(Pauline St.Wharf)	12
25	3	28.38	961	Ft. Morgan, Ala.	32
11	4	28.00	948	Santa Gertrudis, Tex.	6
21	4	28.76	974	Pensacola, Fla.	0
13	3	28.51	966	Pensacola, Fla.	12
8	2	27.44	929	Mean of 2 ships and Dry Tortugas, Fla.	0
20	4	28.65	970	Corpus Christi, Tex.	-
28	3	28.99	982	Houma, La.	10
11	4	29.37	995	Houston, Tex.	33
10	4	28.29	958	Tarpon Springs, Fla.	1
22	4	28.80	975	Hatteras, N. C.	28
29	4	28.71	972	Nantucket, Mass.	12
8	4	-	-	Nr. Dry Tortugas, Fla. (2)	(b)
6	4	29.10	985	Miami, Fla.	0
14	4	29.17	988	Wilmington, N. C.	35
8	4	28.80	975	Merritt Island, Fla.	11
10	4	28.31	959	Houma, La.	3
17	4	27.61	935	Miami, Fla.	4
7	4	28.20	955	Perdido Beach, Ala.	1
16	4	29.16	988	Key West, Fla.	60
13	4	27.62	935	West Palm Beach, Fla.	3
15	2	29.12	986	Pt. O'Conner, Tex.	13
10	4	28.18	954	Long Key, Fla.	7

DATE	P _o in.	P _n in.	P _n -P _o in.	P _o mb.	P _n mb.	P _n -P _o mb.	R n. m. (a)
*Sept. 30, 1929	28.80	29.96	1.16	975	1015	40	58
Aug. 13, 1932	27.83	30.11	2.28	942	1020	78	12
Aug. 4, 1933	28.80	29.96	1.16	975	1015	40	24
Aug. 23, 1933	28.63	29.48	.85	970	998	28	54
Sept. 4, 1933	27.98	29.98	2.00	948	1015	67	13
Sept. 5, 1933	28.02	30.24	2.22	949	1024	75	30
Sept. 16, 1933	28.25	29.82	1.57	957	1010	53	42
June 16, 1934	28.52	29.94	1.42	966	1014	48	37
Sept. 2, 1935	26.35	29.92	3.57	892	1013	121	6
*Sept. 4, 1935	28.71	29.89	1.18	972	1012	40	51
Nov. 4, 1935	28.73	-	-	973	-	-	-
July 31, 1936	28.46	30.00	1.54	964	1016	52	19
Sept. 18, 1936	28.53	29.42	.89	966	996	30	34
Sept. 21, 1938	27.86	29.52	1.66	943	1000	57	50
Aug. 7, 1940	28.76	29.75	.99	974	1008	34	11
Aug. 11, 1940	28.78	30.02	1.24	975	1017	42	26
Sept. 23, 1941	28.31	29.66	1.35	959	1004	45	21
Oct. 7, 1941	28.98	30.19	1.21	981	1022	41	18
Aug. 30, 1942	28.07	29.64	1.57	951	1004	53	18
July 27, 1943	28.78	30.02	1.24	975	1017	42	17
Sept. 14, 1944	27.88	30.66	2.78	944	1038	94	49
*Sept. 14, 1944	28.31	29.39	1.08	959	995	36	26
Oct. 18, 1944	28.02	29.80	1.78	949	1009	60	27
*Oct. 19, 1944	28.42	29.67	1.25	962	1004	42	34
Aug. 27, 1945	28.57	30.13	1.56	968	1020	52	18
Sept. 15, 1945	28.09	30.00	1.91	951	1016	65	12
Sept. 17, 1947	27.76	29.83	2.08	940	1010	70	19
*Sept. 19, 1947	28.53	29.70	1.17	966	1006	40	28
Oct. 15, 1947	28.59	29.65	1.06	968	1004	36	13
Sept. 21, 1948	27.62	29.61	1.99	935	1003	68	7
*Sept. 22, 1948	28.41	29.83	1.42	962	1010	48	16
Oct. 5, 1948	28.85	29.77	.92	977	1008	31	27
Aug. 24, 1949	28.86	30.20	1.34	977	1023	46	24
Aug. 26, 1949	28.16	30.12	1.96	954	1020	66	22
Oct. 3, 1949	28.45	29.95	1.50	963	1014	51	15
Aug. 30, 1950	28.92	29.71	.79	979	1006	27	21
Aug. 30, 1954	28.35	-	-	960	-	-	-
*Aug. 31, 1954	28.38	-	-	961	-	-	45
Sept. 11, 1954	27.97	29.77	1.80	947	1008	61	37
Oct. 15, 1954	27.66	29.55	1.89	937	1001	64	18
Aug. 12, 1955	28.40	29.77	1.37	962	1008	46	45
Sept. 19, 1955	28.51	29.87	1.36	966	1012	46	50
Sept. 23, 1956	28.76	29.83	1.07	974	1010	36	29

Table I - Continued

t _c hrs.	P _a		STATION	r _a n.mi.
	in.	mb.		
4	28.80	975	Panama City, Fla.	6
4	27.83	942	East Columbia, Tex.	0
4	28.98	981	Brownsville, Tex.	15
4	28.66	971	Cape Henry, Va.	16
4	27.98	948	Jupiter, Fla.	0
4	28.07	951	Brownsville, Tex.	2
4	28.25	957	Hatteras, N. C.	7
4	28.52	966	Jeanerette, La.	0
4	26.35	892	Long Key, Fla.	0
-	29.18	938	Columbia, S. C.	30
-	28.73	973	Miami, Fla.	0
4	28.46	964	Ft. Walton, Fla.	0
4	28.52	966	Mean of 2 ships off Hatteras, N.C.	0
4	28.04	950	Hartford, Conn.	7
4	28.87	979	Port Arthur, Tex.	5
4	28.78	975	Savannah WBO, Ga.	2
3	28.66	971	Houston WBO, Tex.	0
4	29.00	982	Carrabelle, Fla.	0
4	28.10	952	Seadrift, Tex.	4
4	28.78	975	Ellington Fld., Tex.	2
4	27.97	947	Hatteras, N.C.	14
4	28.31	956	Pt. Judith, R. I.	3
4	28.02	949	Dry Tortugas, Fla.	4
4	28.42	962	Sarasota, Fla.	1
4	28.57	968	Palacios, Tex.	1
4	28.09	951	Homestead, Fla. (FECRR)	0
3	27.97	947	Hillsboro, Fla.	8
4	28.57	968	New Orleans, WBO, La.	2
4	28.76	974	Savannah, Ga., WBAS	7
4	28.45	963	Key West WBO, Fla.	8
4	28.47	964	Clewiston, Fla.	8
4	28.92	979	Miami, Fla.	2
4	28.86	977	Diamond Shoals L/S, N. C.	3
3	28.17	954	W. Palm Beach WBAS, Fla.	0
4	28.88	978	5 mi. west Freeport, Tex.	7
4	28.92	979	Ft. Morgan, Ala.	0
4	28.35	960	Aircraft Recon.	
4	28.42	962	Suffolk County AFB, RI.	
6	27.97	947	40°N - 71°W Aircraft Recon.	0
4	27.70	938	Little River, N. C.	4
4	28.40	962	Ft. Macon, N. C.	0
4	28.63	970	Cherry Point, N. C.	18
4	28.78	975	Destin, Fla.	2

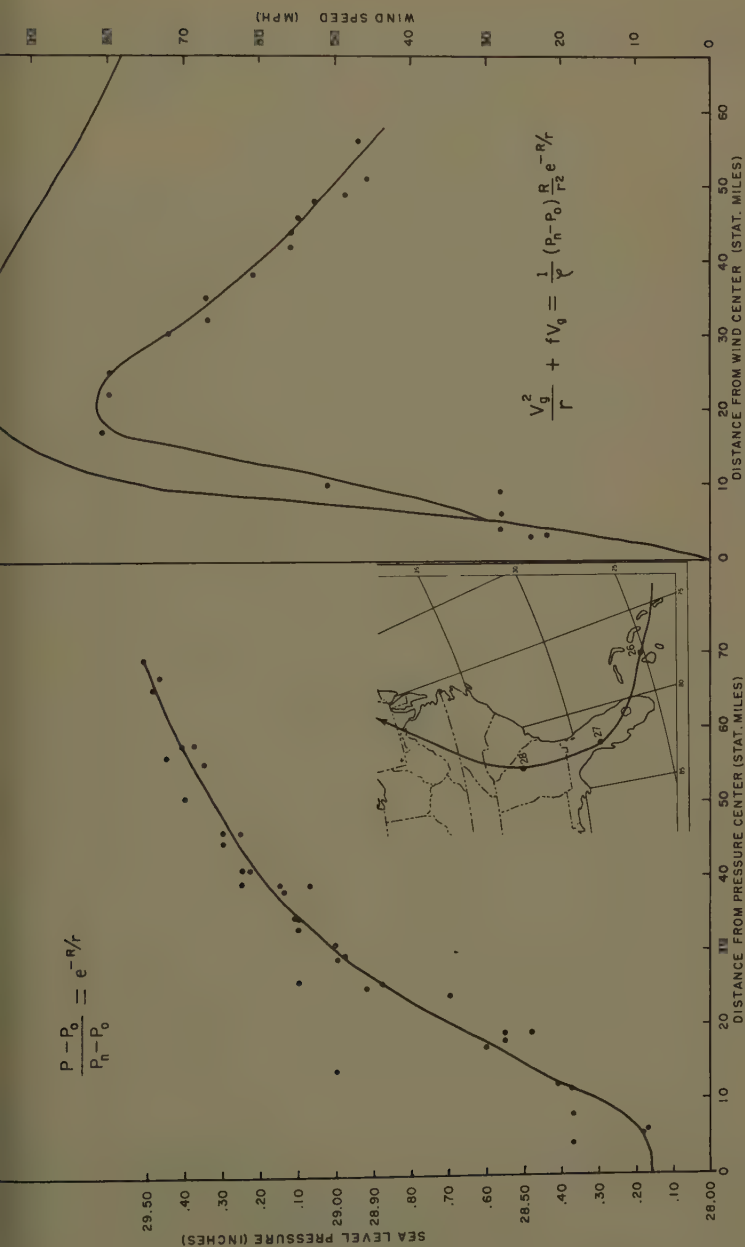
Footnotes for Table I

Note: All values are estimated except p_a .

p_o	central pressure
p_n	asymptotic pressure
$p_n - p_o$	pressure difference between "outside" of storm and center
R	radius to region of maximum wind speed
	(a) computed from pressure profile
	(b) observed from wind speed record
c	forward speed of the storm
t_c	time interval over which storm movement is averaged to obtain c
p_a	lowest pressure detected by a barometer

Station - at which p_a was observed

r_a	minimum distance from station to track of storm center
*	same hurricane as previous line, entering or passing coast at a second point
(1)	Lowest in region where pressure profile parameter were computed 29.31 inches observed at Mobile, Ala. later
(2)	Parameters obtained by interpolating is time between ship off western end of Cuba and Miami, Fla. and apply to vicinity of Dry Tortugas.



Hurricane Aug. 26-27, 1949

Fig. 1. Pressure and Wind distribution in model hurricane.

(4) it is assumed that the winds will blow parallel to the isobars. A more sophisticated theory, as well as observations show that the wind must cross isobars toward lower pressure. The angle of inflow, that is the angle with which the wind crosses the isobars, must be asymmetric with respect to the center of a moving storm. The best determination of the angle of inflow for New England hurricanes is shown as Fig. 2c.⁽⁸⁾

Tides and Storm Surges

If the effects of wind waves and swell are eliminated, the resulting elevation of the sea surface is usually controlled by the gravitational attraction of the sun and moon and the topography of the region of observation. Minor changes of a seasonal nature are also produced by the seasonal changes in atmospheric pressure, prevailing winds, and temperature of the water. The effects of these gravitational and climatic factors can be computed many months in advance and in this paper are identified as the normal tide. In the neighborhood of an intense storm, the actual level of the sea will differ significantly from the normal tide, and the actual level of the sea may be referred to as a storm tide. The difference between the storm tide and the normal tide is called the storm surge.

Economically important storm surges may be produced by extratropical storms as well as hurricanes. Extratropical storms have been responsible for the highest storm tides north of Cape Cod and at a few more southerly locations. However, the surge produced by many hurricanes is much higher than those produced by any extratropical storm. Fig. 3 shows the maximum recorded tide at a representative number of places along the Atlantic and Gulf coasts of the United States.⁽⁹⁾ The remainder of this paper will be devoted to tropical cyclones and the storm tides produced by them.

The peak water level reached in a hurricane will always be somewhat higher than the storm tide level because of the effect of waves with periods of only a few seconds. It is desirable to separate these two phenomena because their effects are quite different. If the peak tide level is two feet above mean sea level, it will penetrate inland to the contour which is approximately two feet above mean sea level, even if this distance is several miles, and it will not rise appreciably above two feet regardless of the slope of the beach. A two foot wave, on the other hand, may run up to a sloping beach to a height of seven or eight feet above the still water line, but under most conditions the effects of such a wave cannot penetrate inland more than a few feet from the still water line, and most of the damage from such waves will be confined to a much narrower strip. The waves which accompany the landfall of a hurricane will generally be in the range of 100 to 1000 feet in length. The remainder of this paper will be restricted to a discussion of the storm surge.

In most cases the principal cause of the storm surge is the frictional drag between the wind and water. Changes in atmospheric pressure, although usually of secondary importance, may occasionally be more important than the wind effect.⁽¹⁰⁾ Waves breaking against the shore or over barrier reefs may contribute to the piling up of water near the shore.

Fig. 4 shows the storm surge produced by Hurricane CAROL at 19 Coast and Geodetic Survey tide stations. The dots on the curves for New London, Groton, and Woods Hole indicate approximate surge heights after the tide

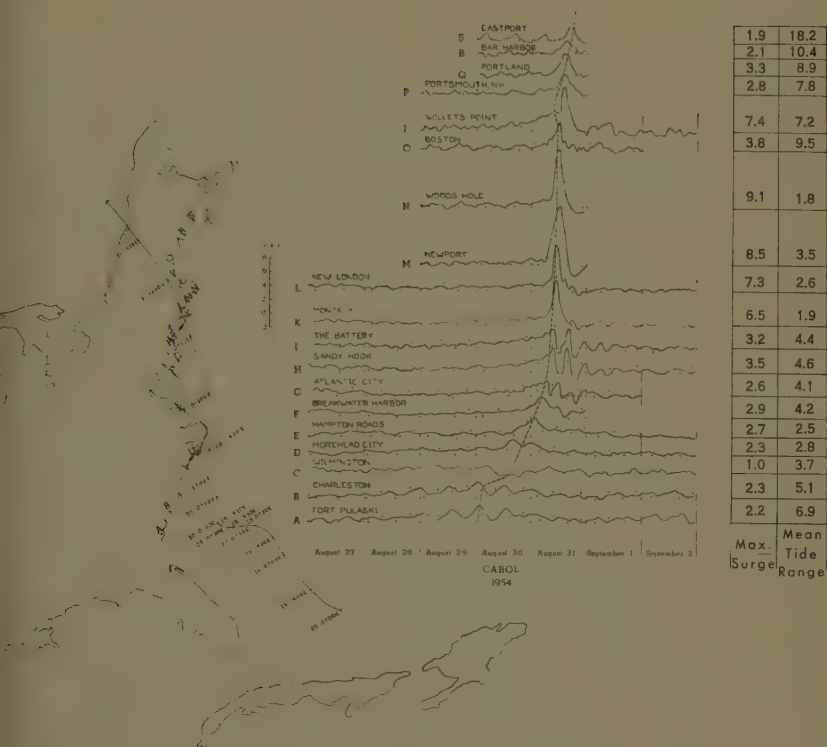
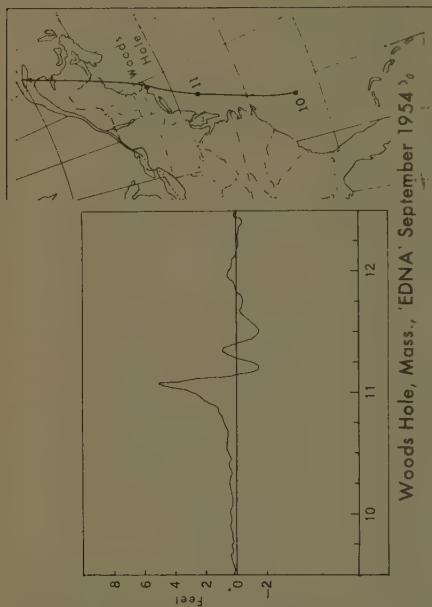


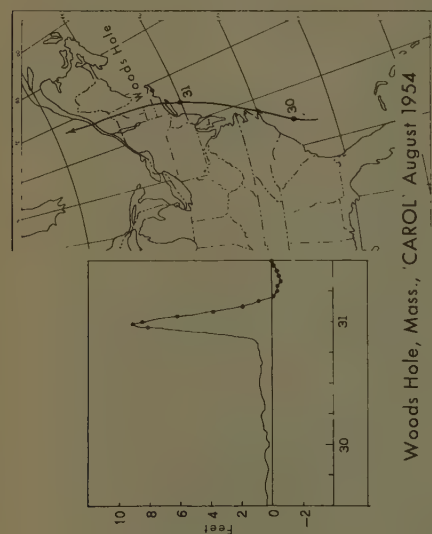
Fig. 4. Track of hurricane and storm surge curves for hurricane CAROL, 1954.

ords of several other stations. These oscillations, called resurgences by field,⁽⁴⁾ are characteristic of the hurricane surge in this region.

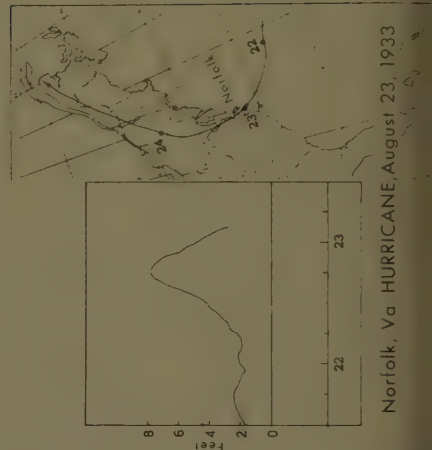
Fig. 5 shows the storm surge as a function of time at the recording tide station nearest the point of maximum storm surge height for several hurricanes. A trend toward rising or falling sea level may become evident 12 to 24 hours before the arrival of the storm. In either, a rapid rise begins when the storm is about 100 to 200 miles distant, that is when the wind speed reaches about 30 miles per hour with the approach of the storm. This period of rapid rise lasts from two to six hours and is generally followed by a slightly more rapid drop to something below the normal water level in areas with good drainage. In marshland or other areas with poor drainage, the water may remain well above normal for several days. Fig. 6 shows the contours of the storm surge along the coast for four hurricanes. Notice the tendency for the peak value to be higher on the right or to extend farther from the center on the right hand side of the storm track. Notice also that the peak storm tide may be as much as 10 feet higher than the storm tide 60 miles to either side of the peak.



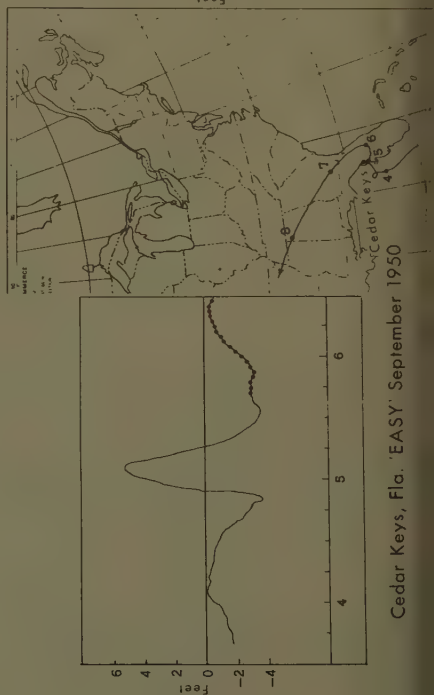
Woods Hole, Mass., 'EDNA' September 1954



Woods Hole, Mass., 'CAROL' August 1954



Norfolk, Va. HURRICANE, August 23, 1933



Cedar Keys, Fla. 'EASY' September 1950

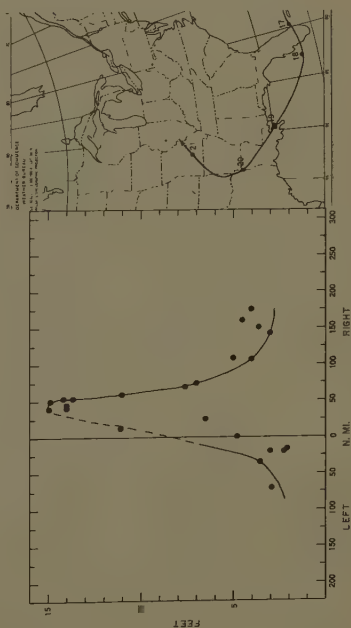
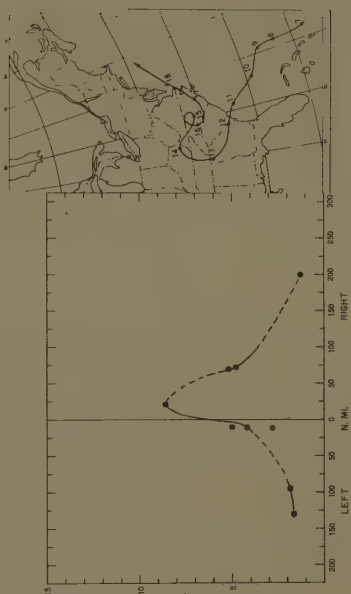
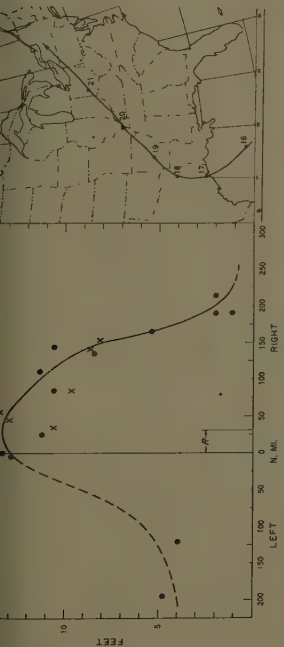
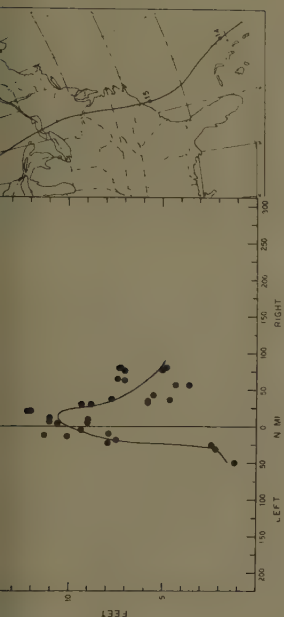


Fig. 6. Storm surge profiles along the coast for four hurricanes.

Fig. 7 based on data furnished by the Corps of Engineers, Coast and Geodetic Survey, Woods Hole Oceanographic Institution and others, shows the storm surge heights produced by Hurricane CAROL at a great many locations along the southern New England and Long Island coasts. Here the effects of topography and local wind conditions are shown by the higher surge heights near the heads of converging bays and at exposed points, and the decreased surge heights near the widest section of Long Island Sound. The varied effects of topography and local wind conditions make it difficult to construct graphs such as Fig. 6, or to develop any relation between storm surge height and meteorological parameters. It is clear that one should avoid using surge heights obtained near the heads of estuaries in developing such relationships, but it is not possible to avoid all local effects.

Maximum Storm Tide as a Function of Storm Intensity

The effect of wind in piling up water is nearly proportional to the wind stress. The wind stress is generally taken as being proportional to the square of the wind speed, and according to Eqs. (2) and (4), this is approximately proportional to the pressure deficiency in a hurricane. The direct hydrostatic effect of the decreased pressure is also proportional to the decrease. Thus, we are encouraged to look for a correlation between $(P_n - P_o)$, or P_o alone, and the maximum storm surge, that is the maximum effect of the storm on the level of the sea. The results of such an effort are shown in Fig. 8.

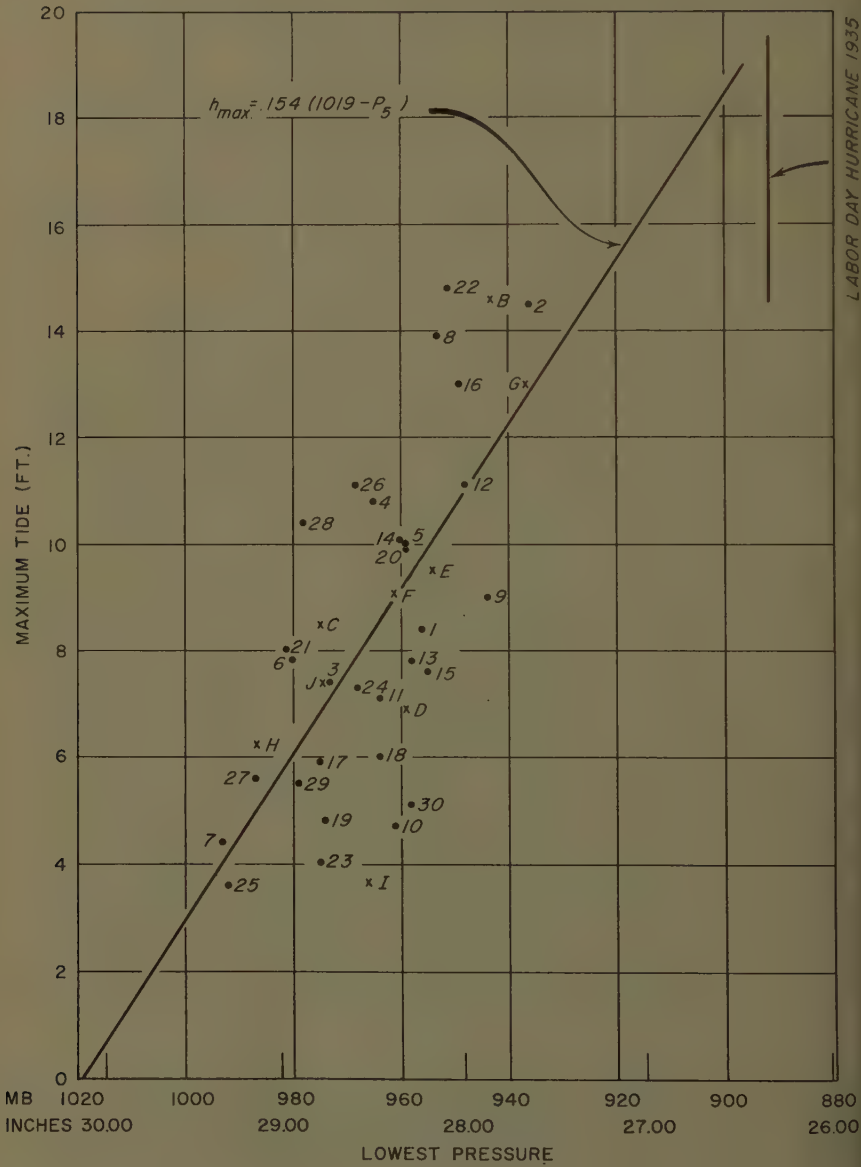
The highest observed tides along the Gulf Coast of the United States during 30 hurricanes is indicated by dots as a function of the central pressure of the storm as it crossed the coast. An attempt has not been made to eliminate the normal tide, as the normal tide range is less than two feet in most of this region, and sufficient data for the elimination of the normal tide were not available for all of the reports. The regression equation based on these data gives a correlation coefficient of 0.68. The extreme differences between the storm and the normal tide for 10 Atlantic Coast hurricanes are indicated by x's. The tide range along the Atlantic Coast is much greater than in the Gulf of Mexico, and a correction for the normal tide is necessary in order to obtain any useful degree of correlation. Largely because of the variability due to the normal tide is eliminated, the correlation coefficient for Atlantic data has been increased to 0.72 even though these data were not considered in the derivation. Consideration of this single parameter is thus sufficient to account for half of the observed variability in maximum storm surge heights.⁽¹²⁾ No improvement was obtained by considering P_n and R as defined in Eqs. (3) and (4), or by using the storm tide potential as defined by Reid.⁽⁶⁾

Effects of the Forward Motion of the Storm

Proudman⁽¹³⁾ using a very elementary theory, has shown that the response of the water in a rectangular canal to a moving atmospheric disturbance could be expressed in the form:

$$h = (1 - V_s^2/gD)^{-1/2} \bar{h} \quad (1)$$





h = height of water level disturbance

\bar{h} = Atmospheric pressure disturbance expressed as the height of a water barometer

V_s = speed of atmospheric disturbance

D = depth of canal

g = acceleration of gravity

Other writers⁽¹⁴⁾ have shown that these results are modified somewhat, when the effects of the earth's rotation and the two dimensional nature of the disturbance are considered. The essential feature of the development which carries over to more complex situations is, that for any basin there is a critical velocity of motion of the atmospheric disturbance which will produce maximum response in the water. An examination of the residuals obtained from Fig. 8 supports this concept, but there are not sufficient data from any type of coastline to establish the proper form of this relationship from empirical evidence.

The speed of the storm can become important in quite another way, for the speed of the storm, together with the radius of maximum winds determines the duration time and the length of the fetch over which the storm winds can act to produce storm tides.

Hurricane Frequency

From a practical point of view, it is necessary to consider the frequency of storms as a function of intensity, size, and region of occurrence. Any real trends in such frequencies would also be highly significant in an economic sense. Unfortunately, the amount of data available for making such studies is rather limited and all data are not of the same quality. The nature and sense of the available data can be indicated by three figures adapted from recent Weather Bureau reports to Congress.⁽¹⁶⁾

Fig. 9 shows the frequencies of tropical storms and hurricanes for the period 1887-1956. A tendency for years of above normal hurricane frequency to be followed by a period of below normal hurricane frequency can be easily noted. There is no evidence of any well marked trend or regular cycle in hurricane frequency. It may be possible to obtain a useful indication of the number of storms to be expected during the next two or three years by considering the number which have occurred during the last 10 to 20 years, but the best estimate of hurricane probabilities more than a very few years in the future would be obtained from considering the frequencies for the entire period of reliable records.

Fig. 10 shows the number of times destruction has been caused by tropical storms on the United States mainland during the present century.

Fig. 11 shows the accumulated frequencies of tropical storms, whose central pressures were 29.00 inches of mercury or less, for several sections of the U. S. Coast. Cape Hatteras is taken as the dividing line between the North Atlantic and South Atlantic sections of the coast for this figure. The data for the Florida Keys are clearly different from those of the other regions. Whether the size of the sample available, nor the present state of theoretical knowledge concerning hurricanes is sufficient to determine whether the

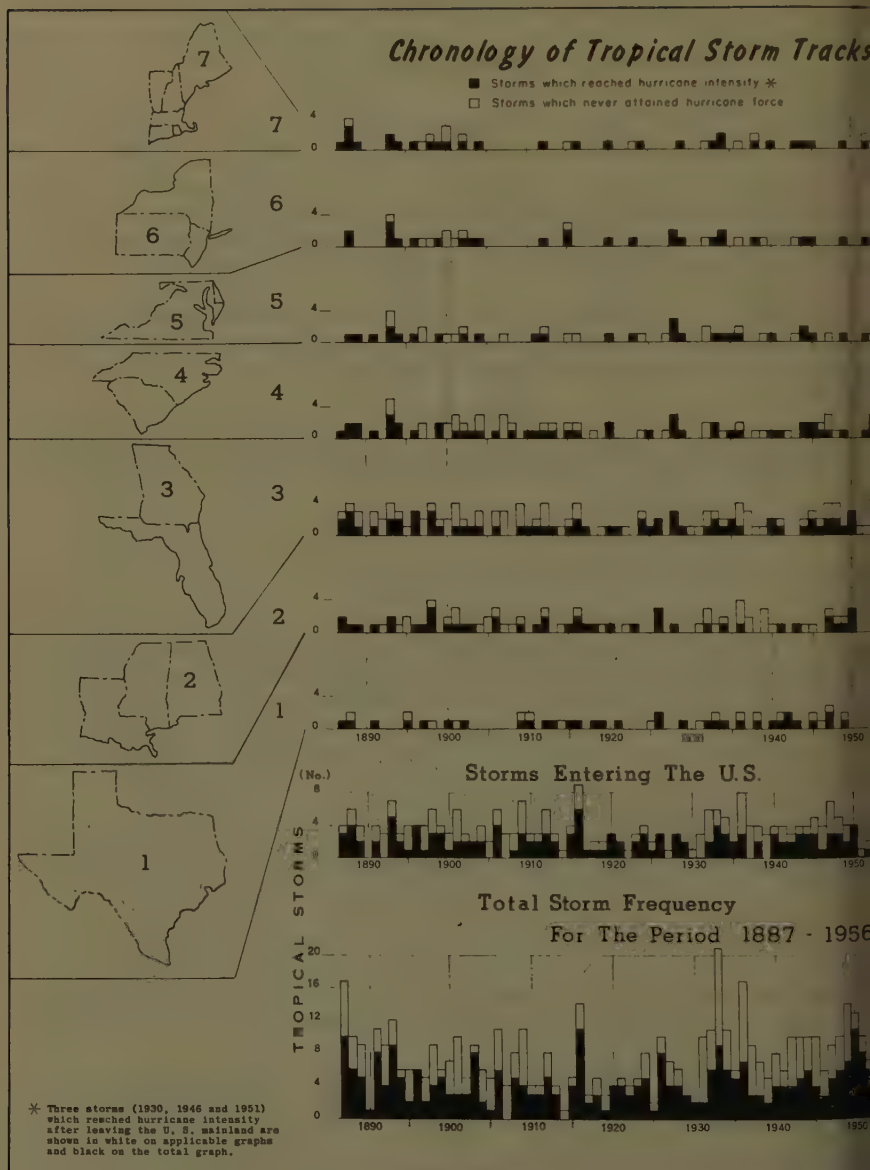


Fig. 9. Chronology of storm tracks. The occurrence of hurricanes and tropical storms in the different coastal regions shown at left, and the total occurrence.

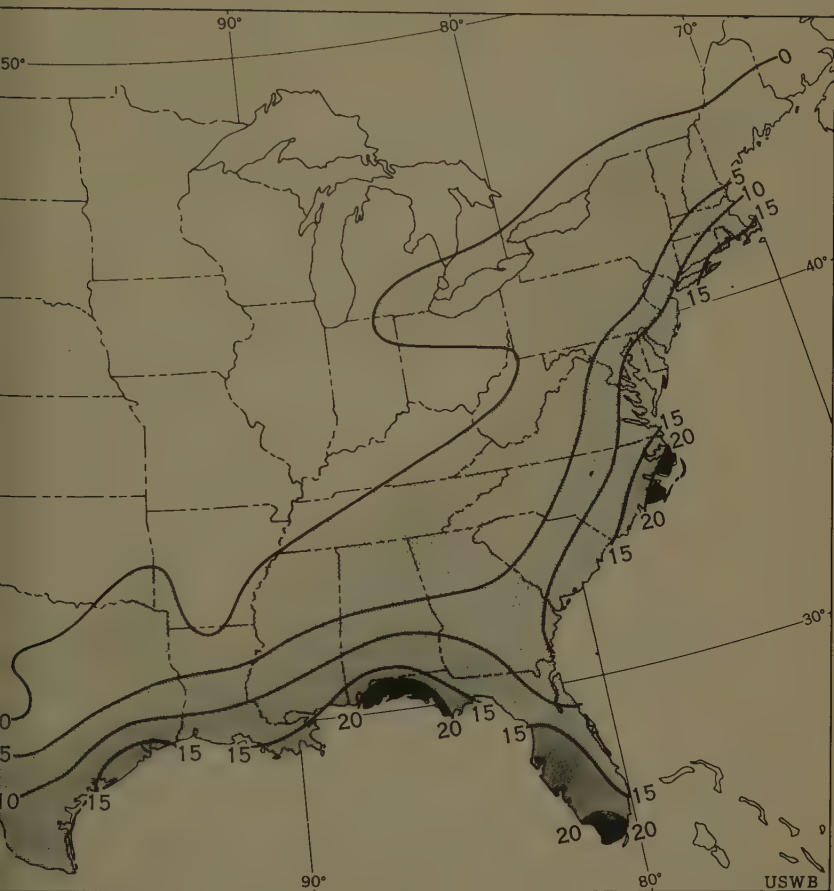


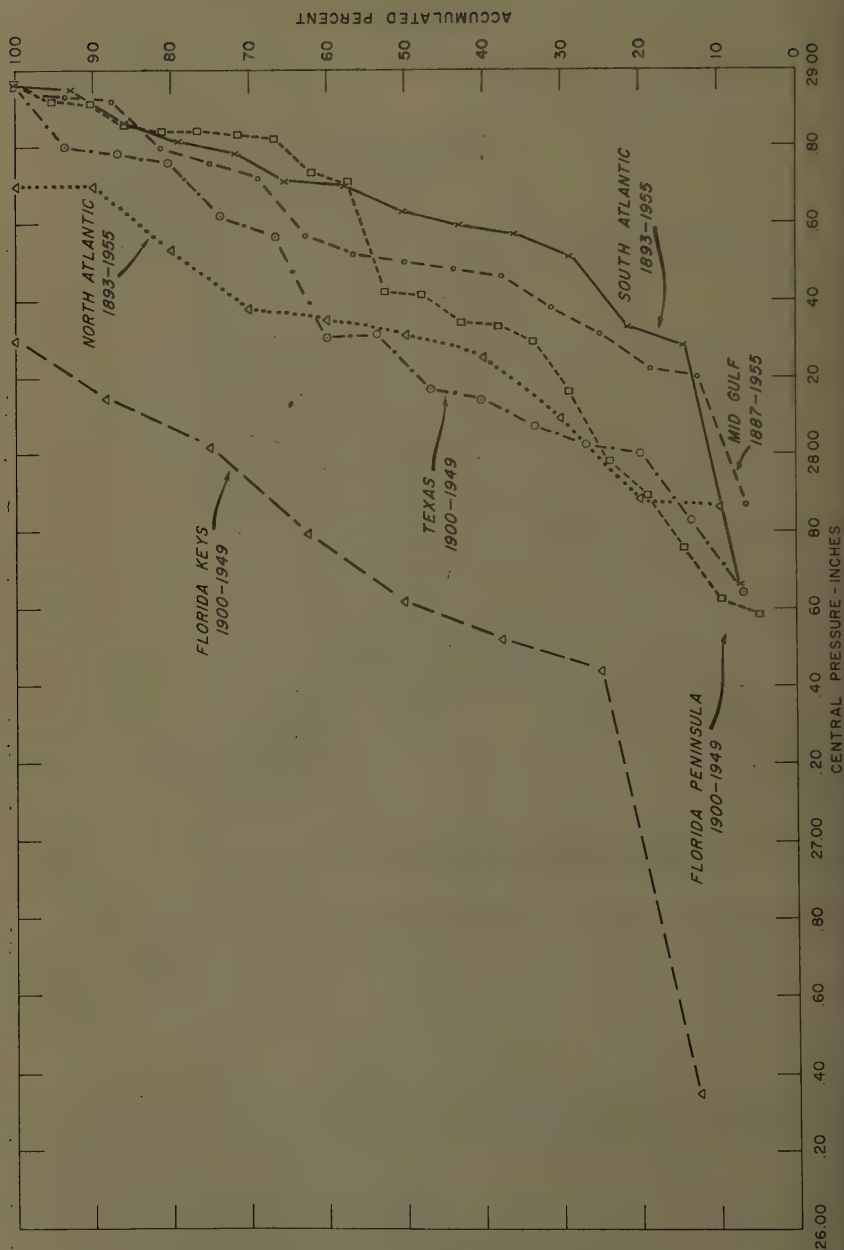
Fig. 10. Number of times destruction was caused by tropical storms, 1901-1955.

ifferences in the other five curves are due to sampling error or to some fundamental aspect of hurricane behavior.

Hurricane Observations and Forecasts

If a hurricane approaches land in the neighborhood of a powerful weather radar installation, such as that now operating at Cape Hatteras, N. C. and on order for about 15 other coastal sites, an experienced radar hurricane observer can locate the center of the storm within 5 to 10 miles while the storm center is within 150 miles of the station. The accuracy decreases as the distance from the radar station is increased.

When the storm is out of range of land based radar, the position of the storm center must be determined from the available ship and aircraft reports.



asionally the eye of the storm will pass directly over a ship. Somewhat frequently, but not on every day of the hurricane's existence, an airplane will penetrate the eye of the hurricane. In these cases the storm center can be located within an accuracy of about 10 miles. In the more usual case, the storm center must be located in the center of an isobaric system determined from fewer than a dozen ship reports, or from radar observations made from aircraft on the edge of the storm. The error in locating the storm center in this way will frequently be as much as 20 or 30 miles and occasionally as much as 60 miles. Errors in communication via radio and teletype further compound the uncertainties resulting from the currently unavoidable shortcomings in our observational procedures.

A few months after the storm, when mailed in reports, free of communication errors, as well as much additional information not available to the forecaster during the storm are obtained, it is possible to repeat the analysis and determine the position of the storm track with an accuracy impossible during the storm.

A simple extrapolation of the storm path accounts for considerably more than half of the obtainable skill in hurricane forecasting. Even the more sophisticated forecast methods, based on a knowledge of flow patterns at all levels, give only a velocity and acceleration of the storm movement, and perpetuate any existing error in the storm position.

When all of these factors are considered, it is evident that storm movements cannot be forecast with timetable accuracy. A study of forecast accuracy for the period 1952 to 1955 indicated an average error of 69 nautical miles in the 12-hour forecast of storm position.⁽¹⁵⁾ This was made up of an average error of 83 miles during the period 1952-1953 and 63 miles in 1954-1955. A gradual improvement in forecast accuracy is to be expected as the result of improved instrument and forecast techniques.

A hurricane watch is announced for specific areas whenever it is recognized that a specific hurricane threat exists for any region of the coast. The hurricane watch is announced before it is possible to delineate the area in which the storm is likely to go inland and when the hurricane effects are believed to be at least 24 hours away from the coast. A hurricane warning is issued for a specific area whenever there exists a reasonable probability that the storm will go inland in that region within the next 24 hours. When the average accuracy of forecasts and the length of coastline seriously affected by a hurricane are considered, it is evident that the hurricane warnings must cover an area several times as large as that which will actually suffer severe damage from the storm.

SUMMARY

A full realization of the hurricane's potential for danger and of the difficulty in predicting its future behavior exactly, should materially reduce the loss of life and property due to these storms.

More than 390⁽¹⁾ persons lost their lives in Hurricane AUDREY, largely because they had lived through other hurricanes with comparatively little damage and did not believe that this storm could be as severe as predicted. Hurricanes vary in intensity. Tropical storms which barely qualify as hurricanes may elevate the sea level no more than four feet, but severe hurricanes may elevate the sea level by 15 feet or more above normal tide for the

time of the hurricane landfall. Intense extratropical storms may produce rises of five to six feet above normal.

The sea level may be raised by one or two feet for a thousand miles of coastline by even a moderately intense hurricane, but the really severe storm surges of more than 5 feet above the normal tide level rarely extend over more than 100 miles of coastline.

The duration of the rapid rise in sea level is rarely greater than 6 hours and in areas with good drainage the fall is even more rapid. In areas of poor drainage, moderately high water may persist for days after the storm.

Knowledge of the intensity of a hurricane before it reaches the coast is meager. The average error in a 12-hour forecast is approximately 60 nautical miles, and if warnings are to be effective, an area several times as large as that actually affected must be alerted.

Disasters such as that which occurred with Hurricane AUDREY can be eliminated by the evacuation of the coastal plain in the threatened region to an elevation of 10 to 20 feet above the normal high water level. In marshland, where high ground may be as much as 40 to 100 miles away by highway, mass evacuations may be required to avoid one catastrophe. With improved instrumentation and forecasting techniques, the number of evacuations, later proved to be unnecessary, will be reduced, but no technique now available will permit the prediction of hurricane motion with timetable accuracy.

BIBLIOGRAPHY

1. H. C. Sumner, "North Atlantic Tropical Storms, 1957", Climatological Data National Summary, Annual, Vol. 8, 1957, pp. 101-113.
2. D. L. Harris, "Some Problems Involved in the Study of Storm Surges," National Hurricane Research Project Report, No. 4, 1956, 30 pp.
3. Bernard D. Zetler, "Hurricane Effects on Sea Level at Charleston," Journal of the Hydraulics Division, ASCE, Paper 1330, August 1957, 19 pp.
4. A. C. Redfield and A. R. Miller, "Water Levels Accompanying Atlantic Coast Hurricanes", Meteorological Monographs, Vol. 2, No. 10, American Meteorological Society, Boston, 1957, pp. 1-23.
5. L. F. Hubert and G. B. Clark, "The Hurricane Surge—An Interim Report," Unpublished research report, U. S. Weather Bureau, Washington, D. C. 1955, 34 pp.
6. Robert O. Reid, "On the Classification of Hurricanes by Storm Tide and Wave Energy Indices", Meteorological Monographs, Vol. 2, No. 10, 1957, pp. 58-66.
7. V. A. Myers, "Characteristics of United States Hurricanes Pertinent to Levee Design for Lake Okeechobee, Florida", Hydrometeorological Report No. 32, Washington, 1954, p. 106.
8. V. A. Myers and E. S. Jordan, "Winds and Pressures Over the Sea in the Hurricane of September 1938", Monthly Weather Review, Vol. 84, 1956, 261-270.
9. D. L. Harris and C. V. Lindsay, "An Index of Tide Gages and Tide Gage Records for the Atlantic and Gulf Coasts of the United States", National Hurricane Research Project Report No. 7, Washington, 1957.

- D. L. Harris, "The Effect of a Moving Pressure Disturbance on the Water Level in a Lake," Meteorological Monographs, American Meteorological Society, Vol. 12, No. 10, Boston, 1957, pp. 46-57.
- R. D. Fletcher, "Computation of Maximum Surface Winds in Hurricanes", Bulletin of the American Meteorological Society, Vol. 36, 1955, pp. 247-250, and V. A. Myers, "Maximum Hurricane Winds", Bulletin of the American Meteorological Society, Vol. 38, 1957, pp. 227-228.
- W. C. Conner, R. H. Kraft, and D. L. Harris, "Empirical Methods for Forecasting the Maximum Storm Tide Due to Hurricanes and Other Tropical Storms," Monthly Weather Review, Vol. 85, 1957, pp. 113-116.
- J. Proudman, Dynamical Oceanography, John Wiley and Sons, New York, 1953, pp. 295-301.
- H. Arakawa and M. Yoshitake, "On the Elevation of the Surface of the Sea Under the Influence of a Traveling Low Pressure Area," Proceedings of the Physics-Mathematical Society of Japan, 3rd Series, Vol. 18, 1936, pp. 51-59; and K. Kajiura, "A Forced Wave Caused by Atmospheric Disturbances in Deep Water," Texas A. & M. Research Foundation, College Station, Texas, 1956.
- U. S. Weather Bureau, "Survey of Meteorological Factors Pertinent to Reduction of Loss of Life and Property in Hurricane Situations," National Hurricane Research Project Report No. 5, Washington 1957.
- Federal Disaster Insurance—Staff Study for the Committee on Banking and Currency, United States Senate, Nov. 30, 1955, 84th Congress, 1st Session Committee Print.

Journal of the
HYDRAULICS DIVISION
Proceedings of the American Society of Civil Engineers

CONTENTS

DISCUSSION
(Proc. Paper 1880)

	Page
mechanics of Sediment-Ripple Formation, by H. K. Liu. Proc. Paper 1197, April, 1957. Prior discussion: 7, 1558, 1832. Discussion closed.)	
by J. Bogardi (corrections)	1880-3
by H.K. Liv (corrections)	1880-3
theastern Floods of 1955: Rainfall and Runoff, by te Dalrymple. (Proc. Paper 1662, June, 1958. Prior ussion: none. Discussion closed.)	
by Howard M. Turner	1880-5

e: Paper 1880 is part of the copyrighted Journal of the Hydraulics Division,
Proceedings of the American Society of Civil Engineers, Vol. 84, HY 7, December,
1958.

MECHANICS OF SEDIMENT-RIPPLE FORMATION^a

 Corrections by J. Bogardi

J. BOGARDI.¹—Corrections to Discussion by J. Bogardi:

Page 1832-3, 14th line "... difficulties to Mr. Liu—of the multitude ..."
 should be "difficulties to Mr. Liu to determine these correlations—of the
 multitude."

Page 1832-4, Eq. (8) " $T_c = U_*^2 =$ " should be " $T_c = \rho U_*^2 =$ ".

Corrections to Closure by H. K. Liu:

Page 1832-29, 16th line "... This factor is proportional to gd/U_*^2 ..."
 should be "The third parameter β is proportional to $d/DS = gd/U_*^2$, the
 channel stability factor, which is the inverse ...".

Page 1832-29, delete (a) the words "in the form" before Eq.(35), (b) Eq.
 (36), and (c) the line following Eq. (35), and substitute the following:

If one uses the channel stability factor $d/DS = gd/U_*^2$ the configuration of
 the bed is quantitatively defined by the parameter β mentioned above unique-
 ly. The relationship of β and gd/U_*^2 according to Bogardi is

$$\beta = \frac{gd}{U_*^2 d^N} \quad (35)$$

From the data of Fig. A, Bogardi assumes that $N \cong 0,882$.

Bogardi further states: Obviously there is a parameter α proportional to
 U_*^2 , which defines the bed configuration uniquely too and

$$\alpha = \frac{d}{(U_*^2)^{1-N}} \quad (36)$$

Finally Bogardi pointed out that a third parameter ϵ proportional to U_*^2
 uniquely defines the bed configuration uniquely too:

$$\epsilon = \frac{U_*^2}{d^{1-N}} \quad (37)$$

α , ϵ and β are obviously interrelated, and their value depends upon the
 temperature, as well as on the specific gravity of the sediment. Assuming a
 temperature of 20° C., and a specific gravity of 2,65, the parameter values
 obtainable directly from Eqs. (35), (36), and (37).

Fig. 19 shows after Bogardi the $U_* = \epsilon d^{\frac{1-N}{2}}$ equations.

Proc. Paper 1197, April, 1957, by H. K. Liu.

Asst. Prof. Technical Univ. of Budapest, Hungary.

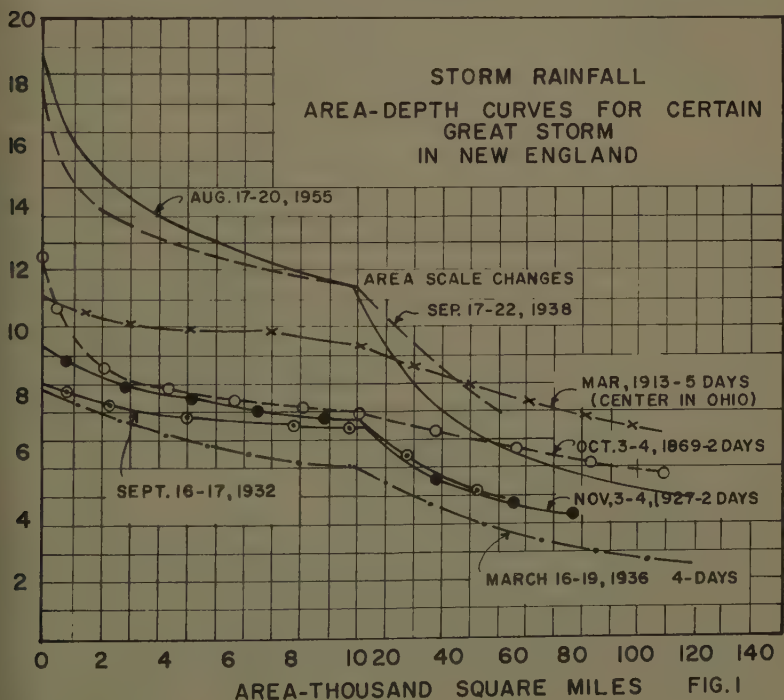
According to Fig. 19 ripples are only possible if $1,777 < \epsilon < 4,06$ and $d < 2\text{mm}$. Bogardi constructed similar figures for Eqs. (35) and (36)."

NORTHEASTERN FLOODS OF 1955: RAINFALL AND RUNOFF^a

Discussion by Howard M. Turner

HOWARD M. TURNER,¹ M. ASCE.—This is a very interesting engineering description of the floods of August and October, 1955. The data selected and presentation of it give an excellent summary of the magnitude and extent of this storm, which, as the author points out, exceeded previous records of intensity of rainfall and flood flows and covered a tremendously wide area. The writer has made some further comparisons of the magnitude of this flood with other large floods in New England.

Fig. 1 shows area-depth curves for total rainfall in various New England storms showing how the 1955 storm exceeded previous records even of the



very large four-day hurricane storm from September 17-21, 1938. Most of the 1955 storm came the two days of August 18 and 19.

The Storm Rainfall report of the Miami Conservancy District, Revised, 1936,⁽¹⁾ gives area-depth curves of great storms in the northeastern part of the country from 1869 to 1933. On Fig. 2 the 1938 and 1955 hurricane storm are plotted on the two-day area-depth curves for the Northeast taken from that report showing how much the 1955 storm exceeded any of these record storms.

It is interesting to compare past analyses of storm intensities with the later records and with the 1955 storm and to note how the results have changed by records which have been added through the years. As an example Fig. 3 shows a curve of high rainfall frequency taken from "The Frequency of High Rates of Rainfall" by Allen Hazen, published in 1921.⁽²⁾ The writer has plotted on this David L. Yarnell's values, published in 1935⁽³⁾ for 10-year and 100-year maxima estimated for Massachusetts and also the maximum actual rainfalls for different periods of time recorded during the 1955 storm. The results of the latter would require an entire recasting of these frequencies derived thirty-six years ago.

In a paper of "Flood Flow Formulas based on Drainage Basin Characteristics" by H. B. Kinnison and B. R. Colby,⁽⁴⁾ a frequency curve of storm rainfall was included. This is shown on Fig. 4. On this are plotted the maximum records for the 1955 storm showing the extreme magnitude of this storm compared with that curve.

It is naturally expected that a longer period of records would have the result of increasing the maximum results obtained, but it is interesting to note

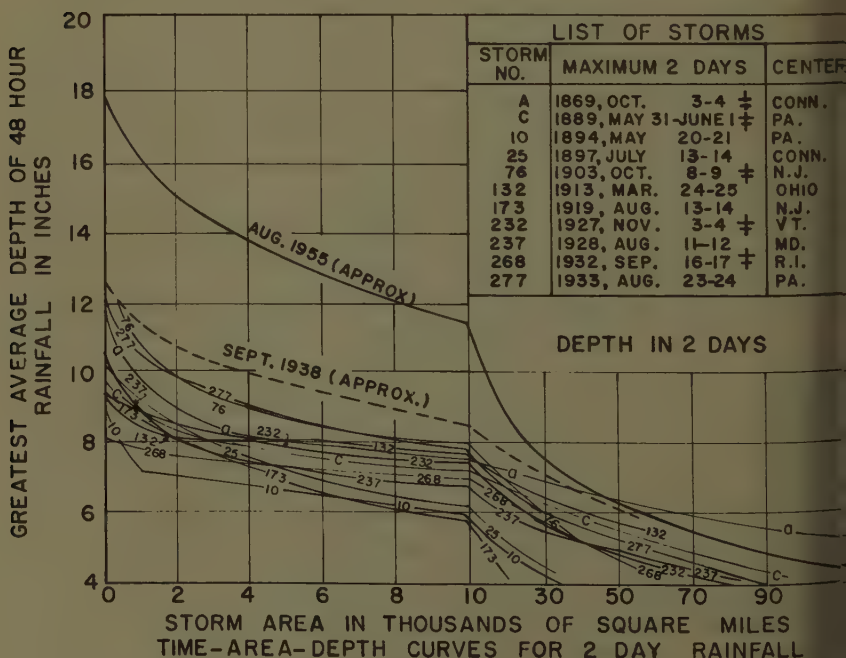


FIG. 2

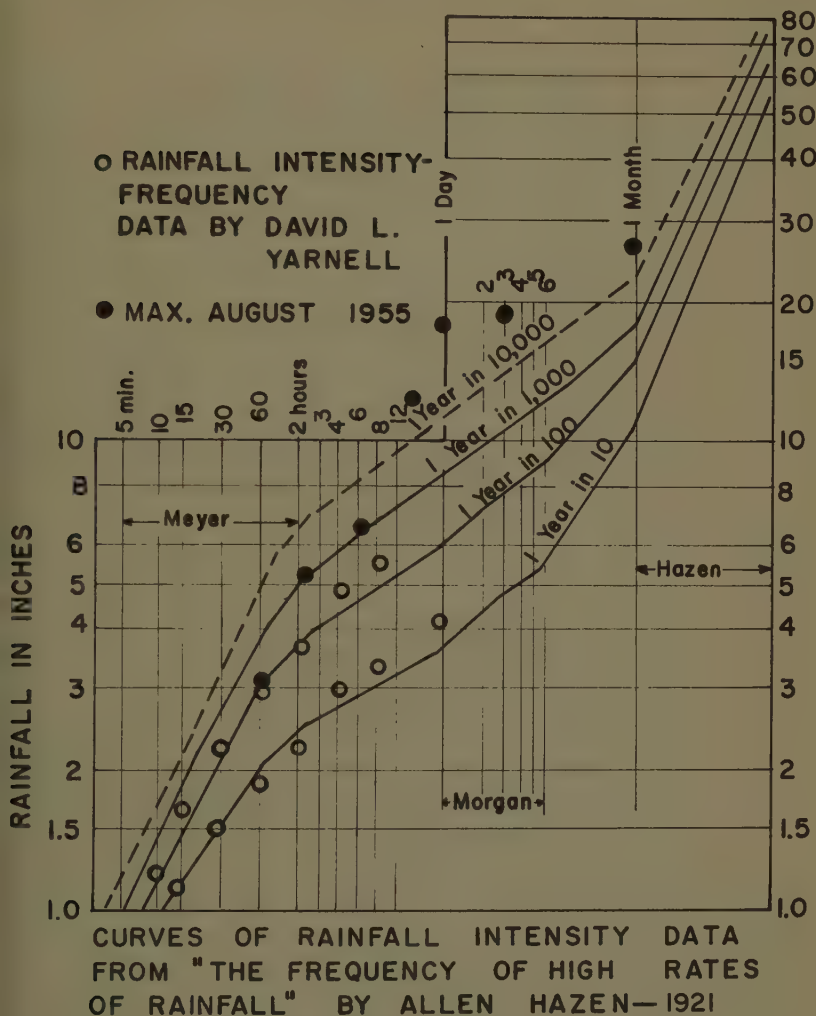
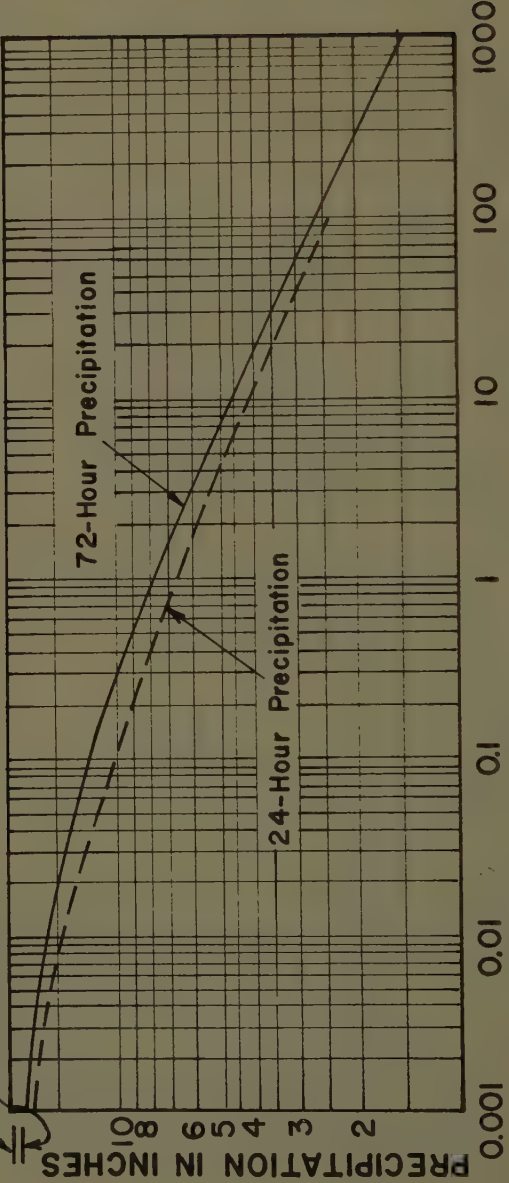


FIG.3

the present period does not seem to show any orderly increase as a long-time of records alone would cause. Fig. 5 shows records of large three-storm rainfall since 1855. The two largest storms have come in the last years, exceeding by 25 per cent anything of record before. Considering flood flows, records of the gage heights on the lower Connecticut River at Hartford are available for the last 114 years. There are a few high-gage records going back for 318 years. The greatest flood in 1936; the next, in 1938; and now the third, in 1955. As far as can be determined from storm and flood histories, nothing of these recent large magnitudes occurred in over 300 years. Fig. 6 shows this large flood record on the Connecticut River at Hartford back to 1683. From all that can be

AUGUST, 1955.
72 Hours = 19.83."
24 Hours = 18.15."



PERCENTAGE PROBABILITY OF OCCURRENCE, IN A YEAR.
FREQUENCY OF 24 & 72 HOUR PRECIPITATION FOR
DRAINAGE BASINS IN MASSACHUSETTS.
CURVES FROM "FLOOD FORMULAS BASED ON DRAINAGE
BASIN CHARACTERISTICS" H.B. KINNISON AND B.R. COLBY.

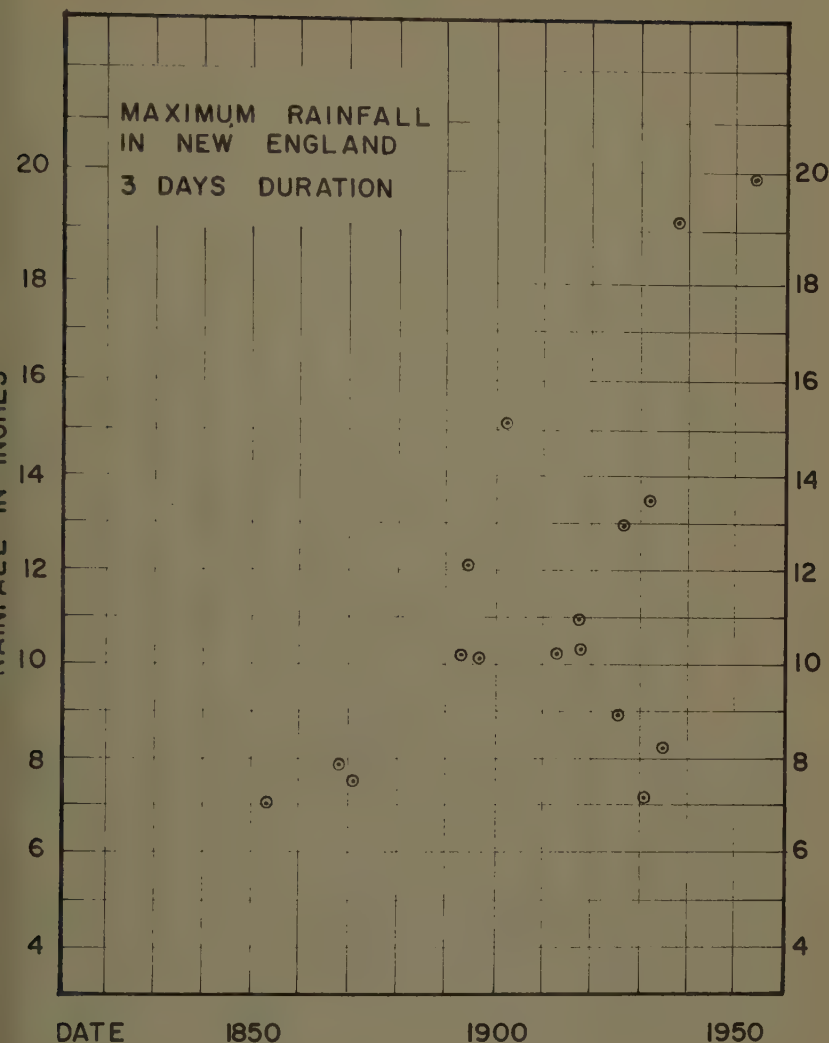


FIG. 5

etermined, the three largest floods have occurred in the last twenty years. The great size of the 1955 storm is shown by the large flood it caused on this river though it was largely confined to the lower third of the drainage area. The author has shown the relation between the peak flow and drainage area as on his Table 5 and Fig. 6. The writer has made up Fig. 7 showing the same data for New England, including the large floods previous to that of August, 1955. A curve of the 40% Myers rating is shown as an enveloping curve including practically all records up to that time. The 1955 flood requires a 70% rating curve to include the high records of the 1955 flood for the drainage areas of 300 to 700 square miles.

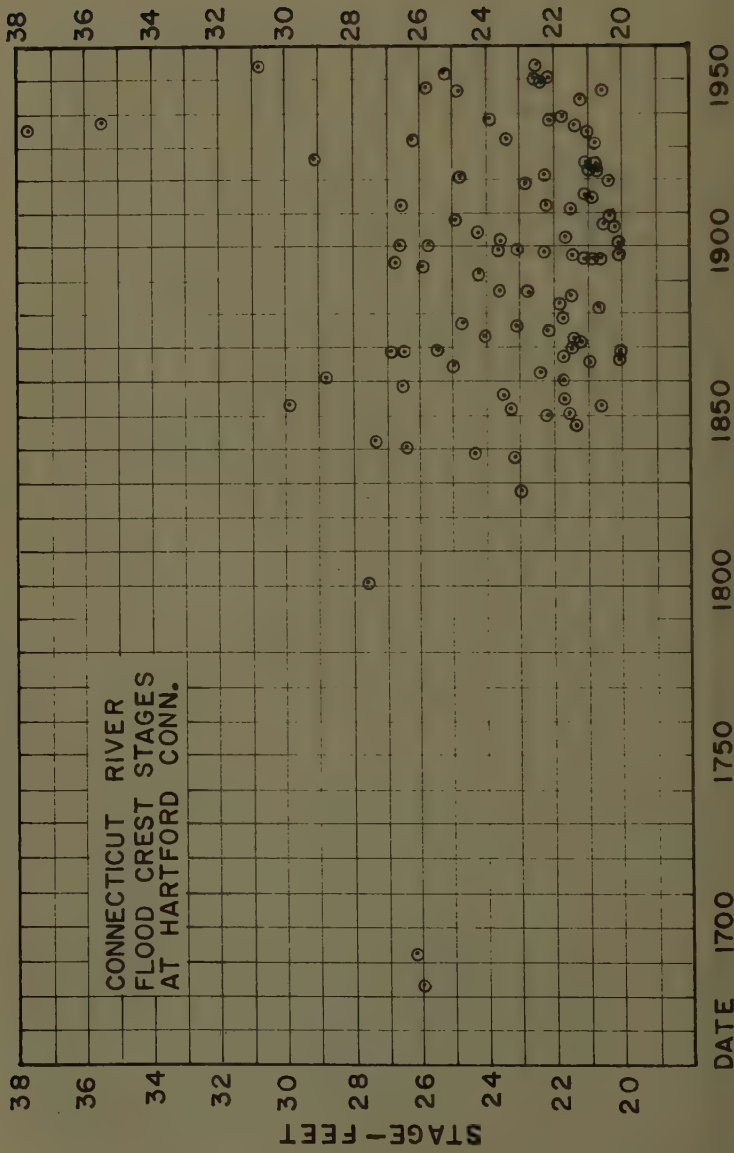
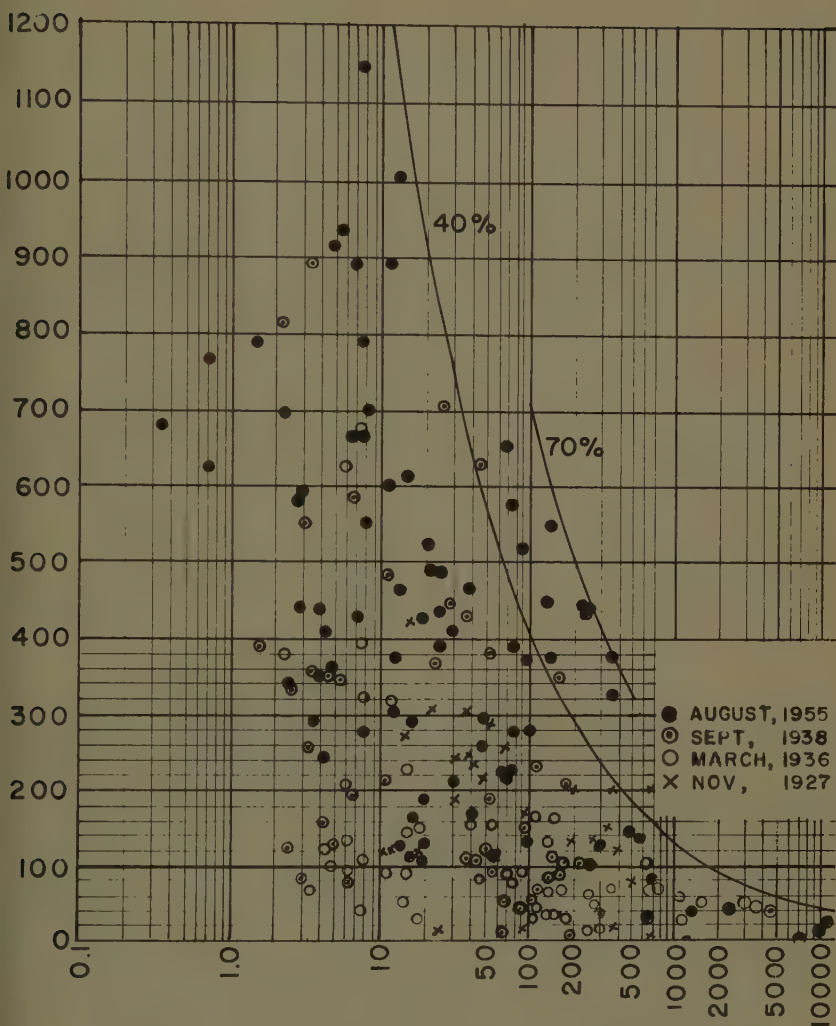


FIG. 6



DRAINAGE AREA IN SQUARE MILES
PEAK FLOWS OF NEW ENGLAND STREAMS
FIG. 7

These very high rates of flow on these fairly small drainage areas shown in the Myers rating and in the rainfall frequency studies are due to the heavy rainfall in a short time. The author shows on Fig. 3 the rainfall curve at Hartford with the total of 14.4 inches in a total time of about 42 hours. Actually 97 per cent of it fell in 28 hours; and about 83 per cent of it, in 24 hours.

Runoff

The author gives some figures of the percentage of runoff to rainfall, which, except for a few cases, appear to be somewhat lower than might be expected from a flood of this intensity. Some of the very high ones that are given may very likely have been affected by the failure of dams.

The author has noted the rapid rise and fall of the hydrographs of this flood. In the case of the large rivers the reason for this is quite evident. For example, on the Connecticut River the heavy storm flows were confined to the lower third of the drainage area. Channel storage was thus confined to only the lower portion of the river valley, and the recession curve of the hydrograph representing the drainage of the channel storage would be shorter in duration as the amount of storage to drain away would not be so great. The same thing shows in the recession limb of the hydrograph of the Delaware River at Port Jervis, where the heavy storm rainfall was concentrated into about 50 per cent of the drainage area.

The hydrographs of the smaller rivers remain to be analyzed. The writer believes, however, that the 6- or 12-hour unit hydrographs for these rivers will prove to be close to the corresponding unit hydrographs for the 1938 flood except that the peaks may be somewhat higher.

Frequency

The question of frequency is one of the most difficult problems in flood studies, but some frequency rating of the size of a given flood seems to be required. The author gives a tabulation and a frequency curve for the Northeast, according to the United States Geological Survey's method of rating the recurrence interval of any given flood as its ratio to the mean annual flood, but the curve gives the recurrence interval up to 100 years only, not long enough for many requirements. This curve shows very different results from that developed for Connecticut by B. L. Bigwood and M. P. Thomas.⁽⁵⁾

The section on flood frequency of the 1942 report of the Committee on Floods of the Boston Society of Civil Engineers, published in 1942,⁽⁶⁾ analyzes the frequency of floods on the Connecticut River at Thompsonville, where there were then over 93 years of record. Various methods were used. The results, using data up to 1935, i.e., prior to the 1936 and 1938 floods, gave a frequency of the 1936 flood from 10,000 to 16,7000 years, depending on the method used. The same computations made with three years' more data including these two large floods gave frequencies from 300 to 400 years.

Apparently the same difficulty is still found by the United States Corps of Engineers as shown in its recent report on the 1955 flood,⁽⁷⁾ where for four rivers in southern New England the flow for a given frequency used in 1955 was much higher than shown by the curves tentatively adopted prior to the 1955 flood. See Table 1.

The paper by Kinnison and Colby, published in 1945,⁽⁴⁾ which has been used a great deal in Massachusetts, rates floods as "minor," "major," and "rare" with stated frequencies of 15, 100, and 1,000 years respectively. On the riv

TABLE I - 1955 FLOOD
COMPARATIVE FLOOD PEAKS AND FREQUENCIES

River	Drainage Area sq. mi.	Maximum Discharge		Ratio Peak Discharge to mean annual flood 1955	Kinnison-Colby (4)		U. S. Corps of Engineers 1955 Flood ⁽¹⁾	
		1938 c. f. s.	1955 c. f. s.		Major 100-year c. f. s.	Rare 1000-year c. f. s.	Frequency in Years Before 1950	After 1955
MASSACHUSETTS AND RHODE ISLAND								
Quinebaug River at Westville	93.8	--	17,500	22.6	5,410	8,970	--	--
W. Br. Farmington R. at New Boston	75.3	18,500	34,300	14.5	12,400	21,900	--	--
Quaboag River at West Brimfield	149	8,470	12,800	11.1	9,410	15,400	--	--
Blackstone River at North Bridge	139	--	16,900	10.9	7,530	12,700	--	--
Kettle Brook at Worcester	31.3	1,300	3,970	7.9	2,860	5,000	--	--
Chicopee River at Indian Orchard	688	45,200	40,500	6.5	36,400*	60,500	--	--
Blackstone River at Woonsocket, R. I.	417	15,100	29,600	5.6	16,600	29,100	3,700	167
Westfield River near Westfield	497	55,500	85,000	--	69,700	111,000	500	77

*. At Bircham Bend 702 sq. mi.

CONNECTICUT

Scantic River at Broad Brook	98.4	11,200	13,300	12.1	- -	- -	- -	- -
Quinebaug River at Putnam	331	20,900	48,000	12.0	- -	- -	See note**	250
Naugatuck River at Naugatuck	246	17,000	106,000	11.8	- -	- -	See note***	264
Willimantic River at South Coventry	123	14,900	46,700	11.5	- -	- -	- -	- -

** Curve gives 2000-year frequency for 32,000 c. f. s.

*** Curve gives 2000-year frequency for 75,000 c. f. s.

on which there are records concerning the 1955 flood, the Kinnison-Colby figures would be as shown on Table 1. These generally rate the higher 1955 flood flows as equal to or exceeding a "rare" flood.

In that paper the flood frequency ratings were based upon precipitation and depth of runoff. The use of precipitation in determining flood frequency has its difficulties because of the varying percentage that occurs in the form of runoff in the flood, but the rainfall data are more inclusive. The writer believes that the flood runoff figures would have some advantage as data for flood frequency computations instead of the peak floods. The runoff data are often not so readily available and require more work to use, but the results are on a broader basis, eliminating the varying characteristics of each stream. With a runoff frequency established, the peak flood of each location could be determined by unit hydrograph methods. On a few of the streams for which Kinnison-Colby figures are available for the high 1955 flood areas the runoff compares to their "rare" or 1,000-year flood.

All this points out the difficulty of the problem. Each of these successive floods gives more information with which to work; but as the author points out in his paper, figures that still show such wide variation are not very "satisfactory." Yet, it is a problem which is important. In over 950 years of records of the flow of the river Danube, the greatest flood was in 1501; the next in 1787 was 85 per cent of it; and the third one in 1899, 75 per cent of it.⁽¹⁾ There is no question but what these extraordinary events occur at wide intervals, and we have to know something of the degree, time, and magnitude in flood works.

Fortunately, frequency is not required so much in the design for spillway capacities of dams except indirectly; but for other designs, such as flood-control reservoirs, flood channel improvements, and other flood-control work, some method is needed to fit the design flood to the value of the proposed construction. The 1955 flood has certainly given perhaps an unsatisfactory but in some ways very convenient yardstick. It has been taken as the design flood on some recent river-improvement designs. As far as the public is concerned, a large storm like that of 1955 is, of course, a very good flood measure. It is much easier to describe flood-control measures for a flood intensity that has already been experienced than it is to talk about the somewhat mythical frequency of a 100- or 1,000-year flood, which may come in the next year.

It is interesting to look back and see the tremendous development of the science of flood analysis and prediction since the 1927 flood. There are still problems, but the progress made justifies the belief that the future will solve them.

REFERENCES

1. "Storm Rainfall of Eastern United States", State of Ohio—Miami Conservancy District, Technical Reports—Part V—1936.
2. "Frequency of High Rates of Rainfall", by Allen Hazen, Engineering News-Record, Vol. 87, No. 21, 1921.
3. "Rainfall Intensity-Frequency Data", by David L. Yarnell, U. S. Dept. of Agriculture—Miscellaneous Publication—No. 204.

"Flood Formula Based on Drainage Basin Characteristics", by H. B. Kinnison and B. R. Colby, ASCE Trans. Vol. 110 (1945), p. 849.

"A Flood Flow Formula for Connecticut", by B. L. Bigwood and M. P. Thomas, U. S. Geological Survey Circular No. 365, Washington, D. C.—1955.

"Journal of the Boston Society of Civil Engineers", Report of the Committee on Floods, Volume XXIX—No. 1—Section 2.

"New England Floods of 1955", Part 2—Flood Discharges, Corps of Engineers, U. S. Army—Office of the Division Engineer, New England Division—Boston, Massachusetts, April, 1956.

Journal of the
HYDRAULICS DIVISION
Proceedings of the American Society of Civil Engineers

EXPERIMENTS ON SELF-AERATED FLOW IN OPEN CHANNELS

Lorenz G. Straub,¹ M. ASCE and Alvin G. Anderson,² A. M. ASCE
(Proc. Paper 1890)

SYNOPSIS

Measurements of distribution of air concentration in self-aerated flows are presented in this paper. The experiments were made in a rough channel and-grain type surface at various slopes and discharges, and the data are used as a basis for study of the mechanism of entrainment of air and to relate the air content and distribution to the characteristics of the flow. The analysis of the data shows that the air distribution can be adequately described by relationships based upon a simplified concept of turbulent transport and thus are functions of the flow characteristics. The maximum depth and mean velocity are both shown to increase above those of a corresponding aerated flow.

INTRODUCTION

A characteristic of high-velocity, open-channel flow is the phenomenon of aeration in which atmospheric air is insufflated into and mixed with the water to create the appearance of "white water" with its violently agitated and defined free surface. This condition is frequently observed in flows down chutes and spillways.

It has been reasonably well established by several observers^(1,2,3) that in flows over a spillway from a quiescent reservoir, incipient aeration does not occur on the slope until a point or region is reached at which the boundary layer thickness is equal to the depth. The characteristic roughening of the

¹ Discussion open until May 1, 1959. To extend the closing date one month, a written request must be filed with the Executive Secretary, ASCE. Paper 1890 is part of the copyrighted Journal of the Hydraulics Division, Proceedings of the American Society of Civil Engineers, Vol. 84, No. HY 7, December, 1958.

² Director, St. Anthony Falls Hydr. Lab., Prof. and Head, Dept. of Civ. Eng., Univ. of Minnesota, Minneapolis, Minn.
³ Associate Prof. of Hydromechanics, St. Anthony Falls Hydr. Lab., Univ. of Minnesota, Minneapolis, Minn.

water surface immediately upstream of the appearance of "white water" can be readily observed in such occurrences. With increasing initial water depths, the points where the surface roughening and the "white water" occur move downstream along with the intersection of the boundary layer with the water surface. These considerations suggest that the aeration phenomena are related to the conditions of turbulence in the flow. Examination of such flow by means of high-speed photography indicates that the upper boundary of the flow is rather ill-defined. It consists of a zone which appears white because of entrained air, while above this zone a spray of water droplets occurs moving more or less parallel to the flow and below which is a region of discrete air bubbles suspended in the fluid. Other investigators have described air-entrained flow as being made up of air bubbles entrained in water in the lower levels and water particles in the air in the upper regions. This concept is further emphasized by measurements of the air concentration distribution^(4,5,6) which show that the air concentration increases continuously from the bed, exhibiting a smooth transition from a finite value near the bed to a maximum value of 100 per cent at the free surface which value is approached asymptotically.

This paper presents the results of systematic experiments on distribution of air in self-aerated flows in a channel set at various slopes and operated at various discharges. A provisional analysis is made of the data with respect to air distribution in a vertical section transverse to the direction of flow with a view of arriving at empirical relationships between concentration parameters and the flow characteristics.

Experiments and Results

Apparatus

The experiments were undertaken in a channel 50 ft. long, 1.5 ft wide, and 1 ft deep, which could be adjusted to any slope from horizontal to nearly vertical. The width was chosen so that for ordinary flows sidewall effects due to growth of the sidewall boundary layer and air entrainment along the sides could be avoided in the central portion of the cross section. That the width was adequate to make the flow two-dimensional in the center portion was demonstrated by earlier measurements of air concentration and velocity in transverse section at the end of the flume.⁽⁴⁾ The flow was obtained by gravity from the laboratory main supply flume through two feed lines and controlled by hydraulically operated valves. The water reached the inlet of the flume through hollow support members and through a rectangular conduit on the underside of the channel. Fig. 1 shows the channel and appurtenances.

At the inlet the flow is guided through two 90-degree vaned bends and a contraction. The inlet gate itself is cantilevered from its mounting at the top of the flume so that there are no slots or guides to disturb the flow. Further guidance is provided by a lip attached to the bottom of the gate and extending inward to further contract the flow; therefore, the gate opening corresponds to the depth of flow at the upstream end of the channel. The maximum gate opening is 0.5 ft. Pitot measurements of the flow just downstream of the inlet with an 0.25-ft gate opening showed no deviation greater than 2 per cent from the mean velocity except in the bottom corners where slightly smaller velocities were encountered.

In the experiments here described, the air-entrainment process was intensified by the installation of artificial roughness on the channel bed that was

siderably rougher than the painted steel sidewalls of the channel itself. The material used for the roughness was a commercial non-slip fabric coat- with granular particles. The particles, whose mean size was 0.028 in., a mean spacing of 0.039 in. and were embedded in a mastic, as shown in 2.

The discharge rate was measured by two calibrated Pitot cylinders mount- in the supply lines and leading to differential gages mounted on the control el. Each discharge meter was calibrated separately for flows from 1/2 0 cfs with an accuracy of the order of 1 per cent.

A control panel contained the actuating components for the hydraulic tem and indicators for the measurement of slope, gate opening, and dis- urge which permitted adjustment of these variables to predetermined es.

The electrical air-concentration measuring instrument has been fully de- scribed in an earlier report.⁽⁷⁾ The method consists basically of a measure- at of the difference between the conductivity of a mixture of air and water and the conductivity of the ambient water alone. A strut supporting a pair of bes is combined with the electrical circuit so that the air-concentration asurements may be made in a small region of the flow. The probes were in. wide and 1/4 in. apart. The instrument is direct reading, and the ation between conductivity and air concentration can be determined ana- cally. The strut holding the probes is arranged so that it is possible to erse the flow cross section both vertically and laterally. The instrument imited to measurements not closer than 0.02 ft from the walls because of rent deflections by the walls at lesser distances. Since the measurements he air concentration depend upon the resistance or specific sensitivity of uspending water, the meter was zeroed in water continually circulated n the test channel through a deaerating tank, thus providing water of the e character as that in the flume. Oscilloscope measurements show a idly fluctuating current between the probes. Since the meter could not ow these rapid fluctuations, the value read on the meter represented an age value. This average compared well with results obtained by means e mechanical sampler which had been previously developed at the Labora- and which was not subject to the same averaging problems. A photograph e probes and strut supports for the air-concentration meter is shown in 3.

Some of the experimental runs also required taking velocity traverses in icals through the aerated flows. The instrumentation for making these ervations has been previously described⁽⁸⁾ in some detail. It consists ntially of a device for timing the travel of minute salt-water cloudlets in- ed into the air-water mixture. The operating principle of the velocity er consists basically of marking a small element of flowing mixture and e recording the time interval required for this marked element to traverse ed distance. The marking is accomplished by making a diminutive portion owing water more highly conductive to electrical current by injecting a ll amount of salt solution into the stream. The passage of this ionized dlet is then detected by electrodes at stations fixed 3 in. apart in the flow . The injections were made at a speed of about 20 per sec with individual ctions of about 0.03 cu cm of 6-per cent saline solution injected in about 0 sec. The accuracy of the air-concentration meter and the velocity er was checked by comparing the measured water rate entering the

channel with the integrated flow determined by the velocity traverses and the air-concentration traverses over the channel cross section.

Experimental Data

For the air-distribution measurements described in this report, the channel slope and water discharge were varied independently. Experiments were made for slopes of 7.5, 15, 22.5, 30, 37.5, 45, 60, and 75 degrees. For each slope, measurements of air concentration were made for total-water discharges from 2.2 to 9.6 cfs and for some slopes up to 15.0 cfs.

The measurements were made at Station 45 (45 ft from the inlet) in a vertical centerline plane. Readings were taken at 0.01-ft intervals on a line normal to the channel bottom with the lowest point 0.02 ft from the bed and the uppermost point where the probes were completely out of the flow and the meter registered zero water concentration. The concentration profile was obtained for each slope and each water discharge after the channel had been adjusted for equilibrium conditions. For this purpose equilibrium flow was considered to be that condition of the flow of the air-water mixture for which the air-concentration distribution was the same at two sections 10 ft apart along the channel. This condition could be obtained by the adjustment of the initial depth of flow through control of the inlet-gate opening. Repeated measurements of the profiles were made at the two sections for different gate openings until the two air-concentration profiles were similar. Comparisons were made of the concentration at corresponding distances normal to the bed. A typical comparison of the profiles at the two stations for equilibrium flow is shown in Fig. 4.

The results of the experiments in the form of measured concentrations for each slope and discharge have been tabulated in Appendix B for reference. A tabulation of computed parameters is given in Appendix C.

The air concentration C is defined as the ratio of the volume of air per unit volume of air and water as measured by the concentration-meter probe. It is assumed that the concentration as measured represents the average value of the concentration in the region described by the probes of the concentration meter and is applicable to the midpoint of the probes. Essentially continuous curves of air concentration with respect to distance normal to the bed were obtained for each experiment. The concentration increases gradually from the bed—more rapidly in the central portion and then more slowly in the upper region, apparently asymptotically approaching the limit of 100 per cent air concentration, as is shown in Figs. 4, 8, and 9. It appears that the complete curve is comprised of two parts which have basically different characteristics. Although there is no sharp demarcation between the two parts, the curves tend to support the description that in the lower regions of the stream air bubbles are suspended in water, while the upper regions consist of water droplets in air. The existence of these water droplets can readily be detected by holding one's hand just above the main flow.

Since there is no definite upper boundary to the air-entrained flow in an open channel, questions of the definition of the linear dimensions of the flow arise. A number of different depth parameters related to the air concentration and distribution may be defined, each having particular applications in describing the bulk-flow conditions. These depth parameters may be described as follows:

- (1) A depth \bar{d} is used to represent a mean depth of flow that would exist if all of the entrained air were removed up to the highest point where water is found. It therefore corresponds to the depth of a nonaerated flow of a given discharge with a velocity equal to that of the entrained flow. It may be defined as

$$\bar{d} = \int_0^{\infty} (1 - C) dy \quad (1)$$

where y is the normal distance from the bed and C is the concentration of air as a function of y . The value of \bar{d} can be approximated with sufficient accuracy by a summation of the products of the water concentrations and their corresponding incremental depths.

- (2) An upper boundary of the air-entrained flow or an upper depth d_u may be defined as the value of y where the air concentration has some arbitrarily prescribed value. For some purposes, such as determining the mean depth, and because of the asymptotic nature of the curve, it is convenient to define d_u as that value of y where the air concentration C is 0.99. Other depths may be similarly defined. Such a depth has previously been defined⁽⁴⁾ as that corresponding to that value of y where the air concentration is $C = 0.95$. This depth was chosen arbitrarily as a depth where the concentration of air can be reliably measured and which includes from 98 to 99 per cent of all of the water and consequently represents a maximum distance from the bed where water will be found.
- (3) A third depth parameter may be defined on the basis of the air-concentration distribution as that depth d_T which represents the value of y where the transition from the distribution in the lower regions to that in the upper regions occurs. Its value would then depend upon the characteristics of the channel as well as the air distribution. This depth parameter will be discussed in detail in a later section.

The mean air concentration in the vertical can also be defined in different ways depending upon the particular application. The mean concentration over the whole range of concentrations measured is defined as

$$\bar{C} = \frac{1}{d_u} \int_0^{d_u} C dy \quad (2)$$

where \bar{C} is the mean concentration of the entire flow and d_u is the so-called upper limit where the concentration is 0.99. Another mean concentration \bar{C}_T may be defined as the mean concentration in the region below the transition depth $y = d_T$ which applies to that air which is being transported by the flow, that is

$$\bar{C}_T = \frac{1}{d_T} \int_0^{d_T} C dy \quad (3)$$

Dimensional plots of \bar{d} , d_u , and d_T for the various discharges and for each slope are presented in Fig. 5 to indicate the range of values as determined from the concentration data. In Fig. 5(c) the mean depth \bar{d} varies with discharge and slope in much the same manner as nonaerated flow. The mean depth increases regularly with the discharge and decreases with the slope. The data for the upper limit d_u (Fig. 5(a)) indicate that for a given discharge d_u tends to decrease at first and then to increase as the slope increases; consequently, the maximum depth tends to be nearly the same for corresponding discharge rates on the various lower slopes. It appears that the increase in depth due to aeration increases with both slope and discharge; however, in combination with the mean depth, which decreases with slope and increases with discharge, the upper limit tends to decrease and then increase as the slope increases. As a result, over a considerable range of slopes (15 to 30 degrees), the upper limit is essentially the same and depends only on discharge. A similar situation exists in regard to d_T (Fig. 5(b)) in that it also shows a tendency to decrease gradually and then to increase gradually as the slope increases. Consequently, the range of variation of d_T for any given discharge is relatively little over a wide range in slopes.

The mean concentration \bar{C} for the entire flow and \bar{C}_T , the mean concentration in the region below d_T , have been plotted in Figs. 6(c) and 6(b) in terms of the discharge and for each slope. It is interesting to note that the mean concentration for the entire flow is nearly constant for a quite wide range of discharges but increases very considerably with the slope. The mean concentration \bar{C}_T for the region below d_T has similar characteristics. In Fig. 6(a) the concentration C_T at the transition depth is plotted. This concentration varies but little with the depth but increases with the channel slope.

Analysis of the Data

Distribution of Air in Aerated Flow

A qualitative concept of air-entrainment phenomena has been established with the aid of the air-concentration determinations made transverse to the direction of self-aerated flows, high-speed photographs and motion pictures of the flow, and other similar information. Since it has been shown that aeration of flows on a steep slope begins in a region where the boundary layer generated by the channel bed has reached the water surface, it is to be presumed that aeration depends primarily upon the turbulence intensity of the flow. Aeration appears to occur when the transverse velocities of turbulence are sufficiently strong near the air-water interface to cause clumps of water to break through the surface into the air and then fall back by gravity into the flowing stream. This breaking away of clumps of water from the main stream and the falling back into the stream with attendant splashing and breaking into a heterogeneous spray of globules and droplets is associated with the insufflation of air into the stream. It occurs particularly with water flow at high velocities on steep slopes. The air carried back is then distributed throughout the flow by turbulent transfer. Observations by means of instruments indicate that two regions of self-aerated flow develop: (1) an upper region of heterogeneous clumps, globules, and droplets of water ejected from the flowing liquid stream into the atmosphere at more or less arbitrary velocities,

(2) a lower region consisting of air bubbles distributed through the flow by turbulent transport fluctuations, which can be described by some boundary-layer equation. Between the two regions is a transition zone defined by a transition depth which is a fluctuating surface necessarily at a statistical mean elevation above the channel bottom.

Distribution of Air in Upper Region

If it is assumed that the components normal to the bed of the turbulent velocity fluctuations are randomly distributed such that the mean value is zero, those in the outward direction will constitute one-half of a Gaussian distribution. Those in or near the surface that penetrate the surface will carry large clumps and smaller globules of water into the atmosphere against the force of gravity a distance proportional to the square of the individual transverse velocities. The maximum height of the trajectories that they follow will also be randomly distributed about zero. (The path will be a long, flat trajectory because of the large, longitudinal component of the local velocity.) If the distances from the surface from which the particles are projected are represented by one half of a Gaussian distribution, the frequency $f(y')$ of particles projected a distance y' above the transition depth may be expressed as

$$f(y') = \frac{2}{h\sqrt{\pi}} e^{-\left(\frac{y'}{h}\right)^2} \quad (4)$$

where h is a measure of the mean distance the particles are projected above the surface. The factor 2 is used to indicate that only particles being projected in the outward direction are being considered; that is, half of the complete Gaussian distribution is being taken so that $\int_0^{\infty} f(y') dy' = 1$. Furthermore, since it is presumed that the flow is uniform on the average, particles are equally likely to be projected at all points of the transitional surface. Then the proportion of all particles leaving a unit area of the transitional surface that reach or pass through a corresponding area at elevation y' will be

$$P_{y'} = \frac{2}{h\sqrt{\pi}} \int_{y'}^{\infty} e^{-\left(\frac{y'}{h}\right)^2} dy' \quad (5)$$

and the number of particles reaching or passing through this area in both directions during the sampling period will be

$$N_{y'} = N_T P_{y'} \quad (6)$$

where N_T is the total number of particles that leave or return to the transition surface per unit area during the sampling period. The average number of particles of water that reach or pass through any horizontal area per unit time may be assumed proportional to the average concentration of water particles. Therefore, using Eqs. (5) and (6), the air concentration at any distance above the transition level in terms of the concentration at the transition level C_T and the representative height h is

$$\frac{1-C}{1-C_T} = \frac{2}{h\sqrt{\pi}} \int_{y'}^{\infty} e^{-\left(\frac{y'}{h}\right)^2} dy' \quad (7)$$

Eq. (7) is, of course, the cumulative Gaussian probability curve and is applicable to the aeration phenomenon only for $y' > 0$. The gradient of the concentration is from Eq. (7)

$$\frac{dC}{dy} = \frac{2(1-C_T)}{h\sqrt{\pi}} e^{-\left(\frac{y'}{h}\right)^2} \quad (8)$$

and when $y' = 0$, $\frac{dC}{dy}$ is a maximum whose value is

$$\left(\frac{dC}{dy}\right)_{\max} = \frac{2(1-C_T)}{h\sqrt{\pi}} \quad (9)$$

and occurs where the concentration is C_T and the depth is d_T .

The constants C_T and h are properties of the flow related to the intensity of the turbulence in the neighborhood of d_T which, in turn, is probably dependent upon the velocity and roughness of the channel.

Distribution of Air in Lower Region

The air entrained at the transition surface by the turbulent fluctuations is then distributed throughout the flow in the region below d_T by the turbulence in the stream resulting in a statistical equilibrium between the bouyancy of the air and the concentration gradient. Such equilibrium is described by the well-known equation

$$-C V_b + \epsilon_b \frac{dC}{dy} = 0 \quad (10)$$

where C is again the air concentration at a normal distance y from the bed; V_b , the rising velocity of the air bubbles, is taken as being negative; and ϵ_b is a mixing parameter for the air-bubble transfer. In aerated flows the value of ϵ_b as a function of y is unknown, and a number of assumptions as to the form of the function can be made. However, it may be presumed that the air bubbles are transported in the same manner as momentum; and it appears reasonable as an approximation to assume ϵ_b to be proportional to ϵ_m , the momentum mixing parameter, as is done in the case of transport of other substances such as sediment. In open channels in the nonaerated condition where the shear is linearly distributed from zero at the surface to a maximum at the bed and the velocity profile is considered to be logarithmic throughout the depth of flow, it has been shown⁽⁹⁾ that ϵ_m has a parabolic form being zero at the surface and at the bed with a maximum at the centerline and can be expressed in the form

$$\epsilon_b = \beta k \sqrt{\tau_o/\rho} \left(\frac{d_T - y}{d_T} \right) y \quad (11)$$

where $\sqrt{\tau_0/\rho} = V_*$, the shear velocity, and τ_0 is the boundary shear at the bottom, ρ is the density of the fluid, β is a proportionality factor in $\epsilon_b = \beta \epsilon_m$, k is the Karman universal constant. In the case of transport in a closed channel, however, the shear at the upper boundary is not zero and the maximum velocity occurs at a point between the upper and lower boundary, at which point the shear is also zero. This requires that ϵ_m also be zero at this point and that the distribution of ϵ_m consists of two parabolas having zero at the boundaries and the point where the maximum velocity occurs, and at the upper boundary and maximum values at intermediate points above and below the point of maximum velocity. It has been shown,⁽¹⁰⁾ however, that suspended matter is actually transported transversely across the level of zero mixing coefficient, and it has been suggested that the mixing coefficient be considered constant in this region. Since it is likely that the vertical transport of suspended matter depends only upon the transverse velocity fluctuations in the vertical direction, such transport may well occur even if the correlation between the vertical and longitudinal fluctuations approaches zero. Measurements of velocity distribution in aerated flows show^(4,5) that the velocity tends to decrease as the upper limit of the flow is approached and that the maximum occurs well down in the flow proper. This implies that a shear is developed in the transition zone. A plausible explanation for such shear is the change in momentum engendered by the return of water clumps and droplets to the flow at the end of their trajectory through the atmosphere above d_T . In the course of that trajectory, they suffer a loss of velocity due to atmospheric drag on the mass. The shear developed at d_T is analogous to the shear at the upper boundary and a distribution of the type found for closed channels might be expected.

The complex distribution found for closed channels may be approximated by a parabolic distribution over the entire region below d_T , with the maximum value incorporated in the factor β . This approximation is equivalent to assuming a distribution for ϵ_b as given by Eq. (11). If this value for ϵ_b , given by Eq. (11), is substituted, Eq. (10) becomes

$$C V_b = \beta k \sqrt{\tau_0/\rho} \left(\frac{d_T - y}{d_T} \right) y \frac{dC}{dy} \quad (13)$$

which upon integration, assuming that V_b is independent of y , is

$$C = C_1 \left(\frac{y}{d_T - y} \right)^z \quad (14)$$

which

$$z = \frac{V_b}{\beta k \sqrt{\tau_0/\rho}} = \frac{V_b}{\beta k V_*} \quad (15)$$

C_1 is a constant whose value is the concentration at $y = \frac{d_T}{2}$.

Application to Experimental Data

The use of Eqs. (7) and (14) as a description of the air-concentration distribution characteristics depends upon the degree to which they fit the experimental data. There are two factors which have a bearing on this: the form of the equation and the magnitude of the constants. Whether or not the form of the equations is reasonably correct depends upon the extent that the assumptions made in their development approximate the actual mechanism. The constants involved depend upon the intensity of the turbulence and at the present cannot be determined analytically but must be evaluated empirically from systematic experimentation.

Eq. (9) permits the determination of the transition depth d_T and the concentration C_T at that depth. From a plot of the concentrations in terms of the normal distance from the bed, the point where the gradient $\frac{dc}{dy}$ is a maximum was graphically located, as shown in Fig. 7(a). The corresponding values of d_T and C_T are noted. Using this value of C_T , the ratio $\frac{(1-C)}{2(1-C_T)}$ was plotted as a function of y on so-called probability paper, upon which a cumulative Gaussian distribution plots as a straight line. The value of h , or rather the value of σ , the standard deviation of the distribution, wherein $h = \sigma\sqrt{2}$, is obtained from the slope of this straight line. Alternately, h can be determined directly from Eq. (9) by evaluating the gradient at the point where $\frac{dc}{dy}$ is a maximum and inserting the value of C_T obtained for that point. Fig. 7(b) shows a plot of the concentrations in the upper region of the flow plotted in this manner with the standard deviation indicated. It is apparent from this plot that the concentrations possess a cumulative Gaussian distribution.

In the region of flow below d_T , Eq. (14) indicated that the concentration C is a function of $\frac{y}{d_T - y}$ which, when plotted logarithmically, results in a straight line whose slope is equal to the exponent z and C_1 is the value of C at $\frac{y}{d_T - y} = 1$. The concentration data for the experiment have been plotted in this manner in Fig. 7 to show the degree of agreement with the form of Eq. (14) and to indicate the evaluation of C_1 and z . Inasmuch as C approaches infinity as y approaches d_T , the experimental data must depart from the curve for the larger values of $\frac{y}{d_T - y}$, but in this case the data agree with the curve up to $\frac{y}{d_T} = 0.9$.

The straight lines drawn through the data in Figs. 7(b) and 7(c) have been transposed to the original plot in Fig. 7(a) to show the characteristics of the curves on the arithmetic scales. Eqs. (7) and (14) have also been plotted along with the data for a number of typical experiments using various discharges and slopes shown in Figs. 8 and 9 for purposes of comparison. Because of the character of Eq. (14) in the neighborhood of $y = d_T$, the two curves are connected by a transition to pass from one curve to the other.

Relation of Parameters to Flow Conditions

Based upon the above analysis of the aeration phenomenon, a number of parameters were developed as being descriptive of both the magnitude and

tribution of the air. These parameters varied with the flow conditions such as the channel slope and discharge, which in turn, along with the roughness characteristics of the channel, govern intensity and scale of the generated turbulence. The flow turbulence is created initially at the bed by the wakes and eddies formed by the flow over the roughness elements; the turbulent eddies are then diffused upward into the flow stream. The intensity of turbulence at the transitional surface which appears to be paramount in the aeration process should then depend upon both the initial generation and the depth of the mixture to the transitional surface. The intensity of the turbulence is related to the boundary shear τ_0 on the bed, which can be expressed by a so-called shear velocity $V_{*b} = \sqrt{\tau_0/\rho}$. Because of the shear that is presumed to exist at the transitional surface, it is not possible in the present experiments to differentiate the bed shear from the total shear. As a first approximation, the total shear or a shear velocity based upon the total boundary shear may be used as a measure of turbulence intensity. To test this hypothesis, the mean air concentration was plotted in terms of $V_*/d_T^{2/3}$ where V_* is defined as

$$V_* = \sqrt{gd_T \sin \alpha} \quad (16)$$

where d_T is the transitional depth previously defined. The expression $V_*/d_T^{2/3}$ is empirical and was chosen as that form which best correlated the data. This plot is shown in Fig. 10. The measured values of the mean concentration correlate reasonably well on a single curve with a tendency for the points corresponding to the smaller discharges to depart from the mean curve. When the mean air concentration in the area below d_T , \bar{C}_T , is considered as being the air concentration which is insufflated and distributed through the flow, the correlation is even better, as shown in Fig. 11. For the higher discharges for each slope the points all fall on a smooth curve, while there is a clear departure from the mean curve for the low discharges on the corresponding slopes. It appears that as discharge decreases below a certain value for a given slope, an additional factor becomes important in reducing the concentration. The nature of this factor is not readily apparent, but it should be noted that a decrease in discharge corresponds to a decrease in d_T , and it is quite possible that an instability in flow pattern arises when the depth becomes small. Considering the data as a whole, it is rather significant that when plotted in this manner, mean air concentrations ranging from about 0.05 to 0.75 corresponding to discharges ranging from about 4 to 15 cfs on slopes with ranges from 7.5 to 75 degrees all correlated along a single curve.

The parameter $V_*/d_T^{2/3}$ includes the depth d_T to the transitional surface. This depth is a function of the air-concentration distribution and is difficult to determine explicitly. It is, however, related to the discharge and slope and is general to the channel roughness. In these experiments the channel roughness is a constant so that for these data, d_T depends only on the slope and discharge. In terms of these measured characteristics, $V_*/d_T^{2/3}$ is related to $S/q^{1/5}$ where $S = \sin \alpha$ and α is the angle of inclination of the bed and q is the unit discharge of water. Consequently, the air concentration that may be expected in a high-velocity open channel can be related to the flow characteristics. This relationship is shown in Fig. 12, where the mean air concentration measured is plotted as a function of $S/q^{1/5}$ for the particular channel in which the experiments were performed. For channels of different roughness characteristics, the curve will probably be similar but shifted an amount to

correspond to the different roughness. A similar plot is given in Fig. 13 showing the mean concentration between the bed and the transitional surface where the depth is d_T . Here again, as in Fig. 11, correlation between \bar{C}_T and $S/q^{1/5}$ appears to be better than that between \bar{C} and $S/q^{1/5}$.

The results shown in Fig. 13 provide a means of estimating the mean air concentration that may be expected in an equally rough, wide open channel of known unit discharge and slope. The depth of flow or the magnitude of the various previously described depth parameters, which are important in design, is a function of the air concentration.

Effect of Entrained Air on the Flow

It was suggested above that the air insufflated into the flow is distributed throughout the flow by turbulent transport. The entrained air has the effect of changing the flow from one of water alone to the flow of a mixture of air and water. Several characteristic depths were defined, such as d_u to represent the uppermost extent of the water particles projected from the flow, d to represent the depth of flow of the water alone, and d_T to represent a new equilibrium depth brought about by the presence of air in the flow. For design purposes, it is of considerable importance to know how these parameters and the actual flow velocity are related to the bulk flow properties or what differences might be expected in these parameters in relation to a corresponding nonaerated flow for which the depth may be computed by means of well-established flow formulas such as the Manning or Chezy formula.

In order to investigate such a relationship, experiments were performed in the experimental channel to establish the resistance of the channel to nonaerated flow, that is, flow of water alone. The slope was decreased so that for comparable discharges the flow would be nonaerated. These slopes ranged from approximately 1 degree to a maximum of about 6.5 degrees, above which aeration was observed to occur. The discharges were in the same range as those used in the aeration experiments. Normal flow was established for each combination of slope and discharge, and the mean depth was determined by averaging the depths measured at various points along the centerline.

The relationship between the depth of flow for the nonaerated condition and the discharge and slope is shown in Fig. 14, where the measured depth d_m is plotted as a function of $q/S^{1/2}$ on logarithmic scales. The equation of the line drawn through the points is

$$q = 90.5 d_m^{3/2} (\sin \alpha)^{1/2} \quad (1)$$

For the range of the variables encountered in the nonaerated flow, it appears that the Chezy formula best describes the data and the coefficient 90.5 characterizes this particular roughness. The mean velocity is then

$$V_m = 90.5 d_m^{1/2} (\sin \alpha)^{1/2} \quad (1)$$

If it were assumed that the same type of flow equation applied to aerated flow, the mean velocity of the air-water mixture flowing at a depth d_T is

$$\bar{V} = C d_T^{1/2} (\sin \alpha)^{1/2} \quad (19)$$

where \bar{V} is the mean velocity of the air-water mixture and C is the Chezy coefficient. Assuming that the velocity of the air and water components are equal, then Eq. (19) can be written in terms of the water discharge, as

$$q = C \bar{d} d_T^{1/2} (\sin \alpha)^{1/2} \quad (20)$$

where \bar{d} is the mean depth computed by Eq. (1) and represents the cross-sectional area of the water. Eq. (20) was tested by plotting the experimental data for aerated flow in the form $\bar{d} d_T^{1/2}$ as a function of $q/(\sin \alpha)^{1/2}$ in Fig. 14. Superimposed upon the plot is the line for nonaerated flow in the experimental channel taken from Fig. 14. The data cluster about the straight line for nonaerated flow, indicating that an equation similar to Eq. (20) will correlate the data, and, in addition, when the parameters \bar{d} and d_T are used, the Chezy resistance coefficient is essentially the same as that for nonaerated flow. Fig. 15 shows that at least for the conditions of these experiments, air-entrained flow, when considered to be a flow of a mixture, follows the same laws as for nonaerated flow when depth parameters related to the properties of the mixture are used to define the linear flow dimensions. The agreement of the data for aerated and nonaerated flow shown in Fig. 15 substantiates somewhat the deductions made in regard to the air-entrainment process. An evaluation of \bar{d} , d_T , and d_u for specific flow conditions is not possible from Fig. 15. A clearer idea of the changes in these parameters will be obtained if they are compared with the depth d_m computed in the usual manner, using Eq. (17) which includes for this channel the Chezy coefficient of 90.5. d_m is the depth at which the water would flow in this channel at the given discharge and slope assuming no air entrainment. The ratios d_u/d_m , d_T/d_m , and \bar{d}/d_m as functions of mean air concentration are plotted in Fig. 16(a), 16(b), and 16(c). In all cases, of course, the ratios approach unity as the air concentration approaches zero. That is, for water flow only, $\bar{d} = d_T = d_m$. As the mean air concentration increases, the ratios depart from unity in such a way that as \bar{C} approaches 1.0, \bar{d} becomes very small, while d_u and d_T necessarily increase.

The upper limit of the spray d_u increases very considerably with increased air concentration which in turn means an increase in the turbulence intensity to project water particles farther into the atmosphere. For the highest air concentrations measured, the value of d_u is nearly four times as large as the aerated depth for a corresponding discharge and slope. The transition depth, as might be expected, also increases relative to the computed depth with increasing concentration bulks the flow and makes the effective depth smaller. On the other hand, the mean depth decreases with increasing concentration. It appears from Fig. 16 that air concentration has relatively little effect on d_T and \bar{d} until the air concentrations are greater than about 50 per cent. For the slopes where the air concentrations were the greatest (being about 85 per cent), \bar{d} was reduced to about one half of d_m while d_T was nearly twice as large as d_m .

The decrease in \bar{d} with increase in mean air concentration implies a corresponding increase in the mean water velocity above that computed on the basis of d_m since \bar{d} is the cross-sectional area of the water flow. The trend of the

mean water velocity in terms of the nonaerated velocity in this channel is shown in Fig. 17. Here again, the velocity of aerated flow is about the same as that of a corresponding nonaerated flow until the mean concentration is in the neighborhood of 50 per cent. It then increases rather rapidly.

CONCLUSIONS

1. Self-aerated, high-velocity, open-channel flow appears to consist of two distinct phases: an upper region consisting primarily of independent droplets and larger agglomerations of water that move independently of the stream proper, and a lower region in which discrete air bubbles are suspended in a turbulent stream and are distributed by the mechanism of turbulence.

2. In the upper region, the distribution of water-air agglomerate and droplets can be adequately described by the Gaussian cumulative probability equation, the constants of which are properties of the flow conditions. In the lower region, the distribution of the air agrees closely with an equation for turbulent mixing based upon an approximation for the distribution of the mixing parameter.

3. The magnitude of the entrained air concentrations apparently depends upon the intensity of turbulent fluctuations generated at the rigid bed and the depth of flow. The mean concentration could be correlated with the parameter $V_* / d_T^{2/3}$ or in terms of the flow characteristics; the mean concentration \bar{C} is a function of $S/q^{1/5}$, where S is the sine function of the slope angle, and q is the unit discharge.

4. The maximum height of water (or spray) above the rigid bed relative to a corresponding nonaerated flow increases rapidly with mean air concentration in the flow. The transition depth is greater than the depth of a corresponding nonaerated flow because of the bulking effect of the entrained air.

5. The mean velocity of an air-entrained flow is greater than that of a corresponding nonaerated flow by an amount that increases with the air concentration and corresponds to a decrease in the mean depth.

6. When the effective depth of aerated flow is taken to be the transition depth and the mean depth is the cross-sectional area per unit width of channel, the flow is described by a formula of the Chezy type involving approximately the same roughness coefficient as applies for nonaerated flow in the same channel.

ACKNOWLEDGMENTS

The experimental results reported here were developed as part of a program of investigation on the basic mechanics of atmospheric air insufflation and entrainment by water flowing at high velocity with a free surface. The study was sponsored by the Office of Naval Research at the St. Anthony Falls Hydraulic Laboratory of the University of Minnesota. Alan S. Goodyer and Jimmie F. Hayek, research assistants at the time of this phase of the program, assisted in the collection and analysis of the data.

LIST OF REFERENCES

1. Lane, E. W., "Entrainment of Air in Swiftly Flowing Water." Civil Engineering, Vol. 9, No. 2, pp. 88-91. February 1939.

- Hickox, G. H., "Air Entrainment on Spillway Faces." Civil Engineering, Vol. 15, No. 12, pp. 562-563. December 1945.
- Halbronn, G., "Étude de la Mise en Régime des Écoulement sur les Ouvrages a Forte Pente." Thesis submitted to the University of Grenoble, Grenoble, France. 1951.
- Straub, Lorenz G. and Lamb, O. P., "Experimental Studies of Air Entrainment in Open Channel Flow." Proceedings, Minnesota International Hydraulics Convention, Minneapolis, Minnesota, pp. 425-437. September 1-4, 1953. (Also Transactions, American Society of Civil Engineers, Vol. 121, pp. 30-44. 1956.)
- Halbronn, G., and Cohen de Lara, G., "Air Entrainment in Steeply Sloping Flumes." Proceedings, Minnesota International Hydraulics Convention, Minneapolis, Minnesota, pp. 455-466. September 1-4, 1953.
- Viparelli, M., "Flow in a Flume with 1:1 Slope." Proceedings, Minnesota International Hydraulics Convention, Minneapolis, Minnesota, pp. 415-423. September 1-4, 1953.
- Lamb, O. P. and Killen, John M., An Electrical Method for Measuring Air Concentration in Flowing Air-Water Mixtures. University of Minnesota, St. Anthony Falls Hydraulic Laboratory Technical Paper No. 10, Series B. March 1952.
- Straub, Lorenz G., Killen, John M. and Lamb, Owen P., "Velocity Measurements of Air-Water Mixtures," Transactions, American Society of Civil Engineers, Vol. CXIX, pp. 207-220. 1954.
- Vanoni, Vito A., "Transportation of Suspended Sediment by Water." Transactions, American Society of Civil Engineers, Vol. CXI, pp. 67-133. 1946.
- Ismail, Hossan M., "Turbulent Transfer Mechanism and Suspended Sediment in Closed Channels." Transactions, American Society of Civil Engineers, Vol. CXVII, pp. 409-446. 1952.

LIST OF SYMBOLS

- C - Concentration, ratio of volume of air to volume of air plus water.
- \bar{C} - Mean concentration in vertical section.
- C_1 - Concentration at point $y = d_T/2$.
- \bar{C}_T - Mean air concentration in region between lower boundary and d_T .
- C_T - Concentration at transition depth $y = d_T$.
- \bar{d} - A mean depth of flow defined by Eq. (1).
- d_u - Upper limit of flow or value of y where $C = 0.99$.
- d_T - Transition depth between upper and lower regions of flow.
- d_m - Mean depth in nonaerated flow.
- g - Acceleration due to gravity.

- h - A mean height to which water particles are projected above d_T .
- k - Von Karman universal constant for velocity distribution.
- $N_{y'}$ - Number of particles reaching or passing through a horizontal area at a distance y' above transition depth d_T .
- N_T - Number of particles that leave or return to an area at the transition depth.
- $P_{y'}$ - Proportion of all particles leaving area at transition depth that reach or pass through horizontal area at y' above transition depth.
- Q - Total-water discharge.
- q - Water discharge per unit width of channel.
- V - Local velocity.
- \bar{V} - Mean velocity in vertical section = $q/d(\bar{d})$.
- V_* - Shear velocity = $\sqrt{g(d_T) \sin \alpha}$.
- V_b - Rising velocity of air bubbles.
- y - Normal distance from channel bottom.
- y' - Outward normal distance above transition depth.
- z - Exponent in air-concentration equation.
- α - Angle of inclination of channel.
- β - Constant.
- ξ_b - Mixing coefficient for air bubbles in turbulent flow.
- ξ_m - Mixing coefficient for momentum transfer.
- ν - Kinematic viscosity of water.
- ρ - Density of water.
- σ - Standard deviation of air distribution above d_T .
- τ - Local shear force.
- τ_0 - Boundary shear force.



Fig. 1 - Variable Slope Channel for Air-Entrainment Experiments



Fig. 3 - Probes for Air-Concentration Measurements



Smallest scale division equals $1/64$ inch

Fig. 2 - Artificial Roughness Elements Installed on Channel Bed

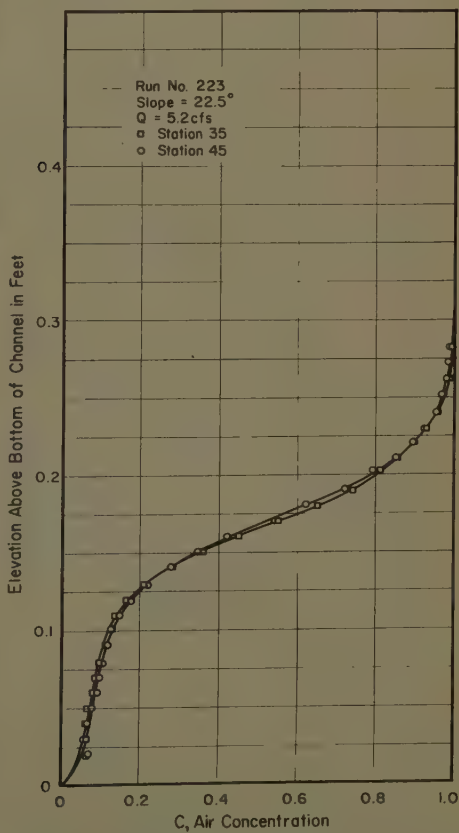


Fig. 4 - Comparison of Air-Concentration Profiles at Stations 35 ft and 45 ft From Inlet

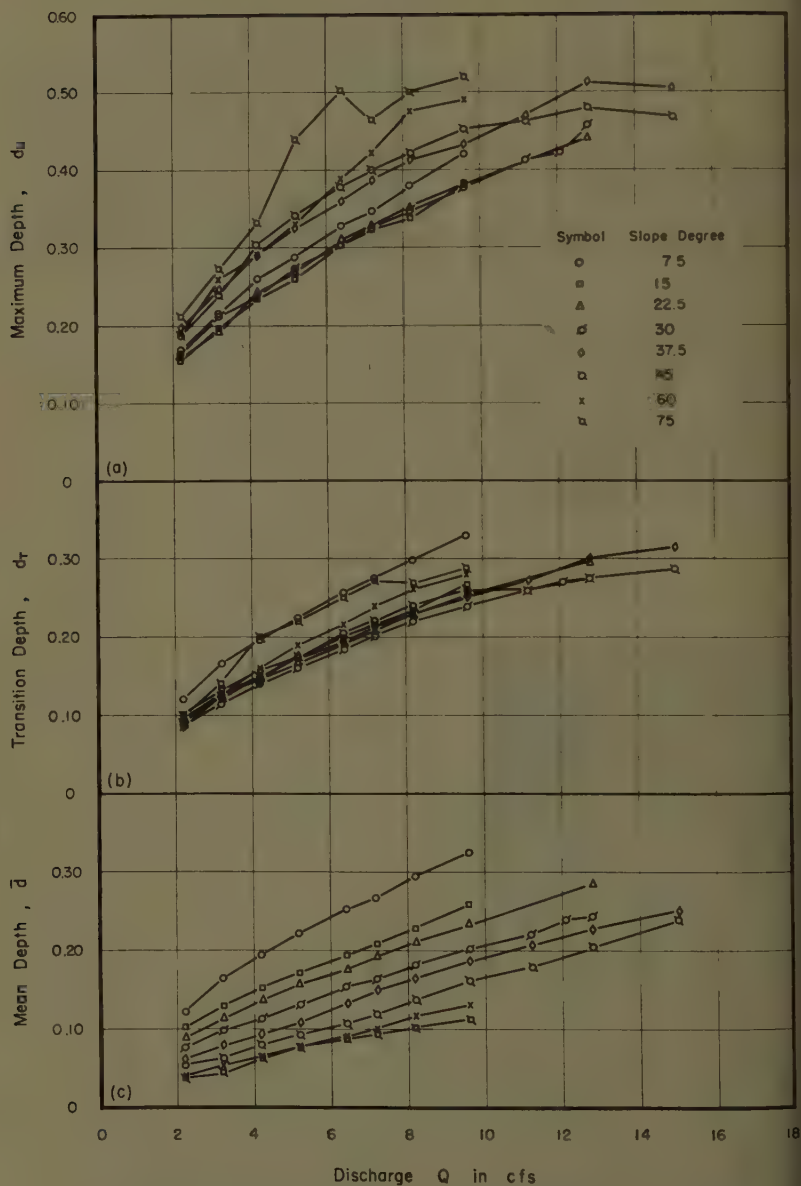


Fig. 5 - Depths of Aerated Flow as a Function of Discharge; (a) Upper Limit, d_u ; (b) Transition Depth, d_T ; and (c) Mean Depth, \bar{d}

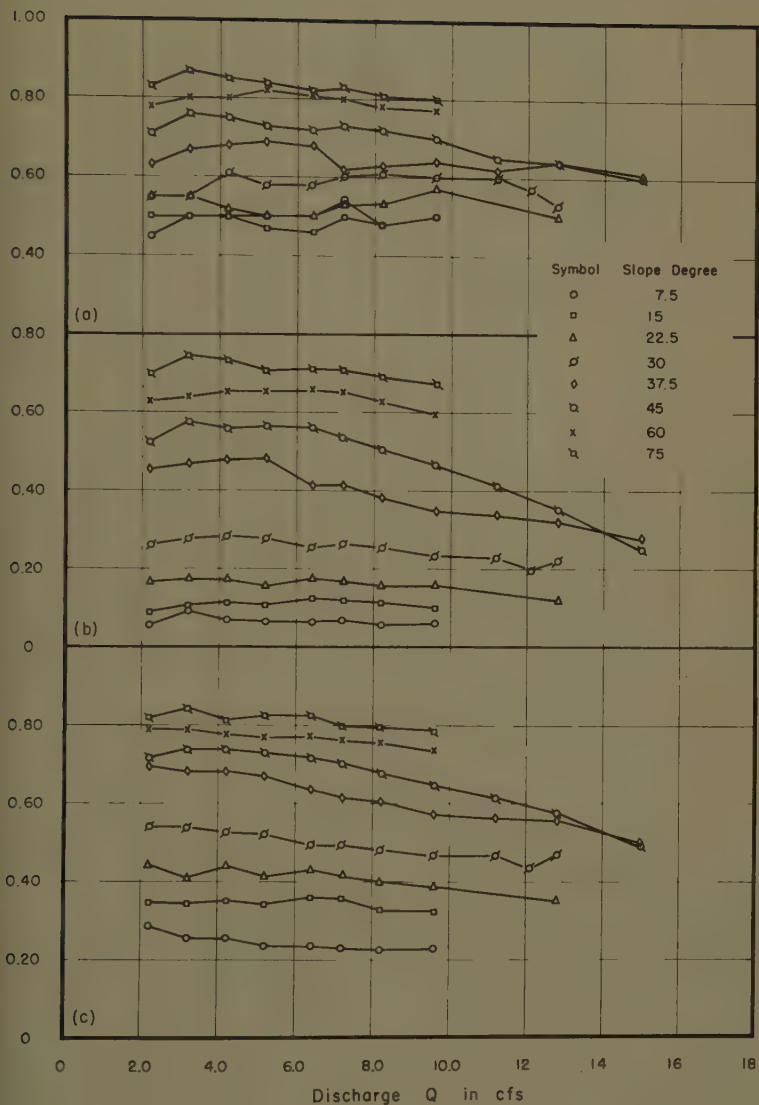
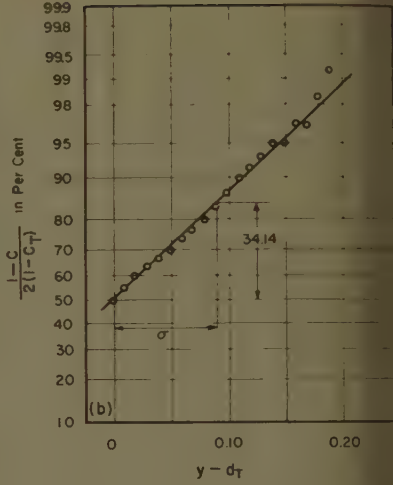
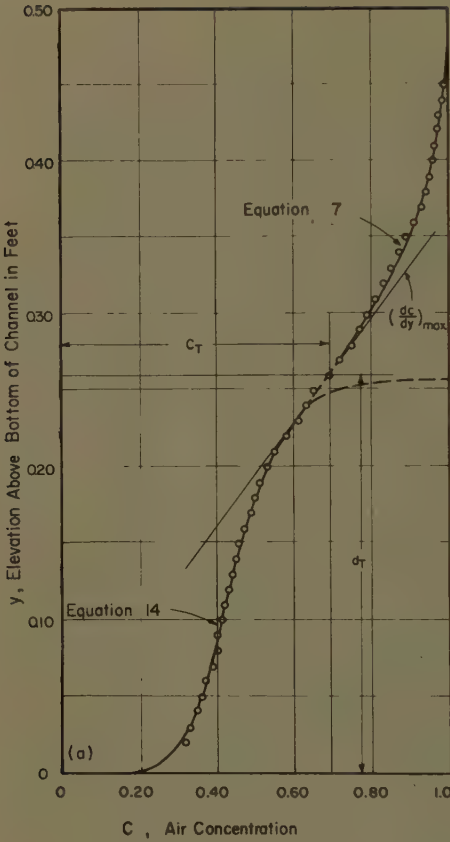


Fig. 6 - Air Concentrations as Functions of Slope and Discharge



Run 257	
Slope	= 45°
Q	= 9.6 cfs
d_T	= 0.260
C_T	= 0.70
σ	= 0.090
C_s	= 0.453
z	= 0.143
\circ	= Experimental
/	= Theory

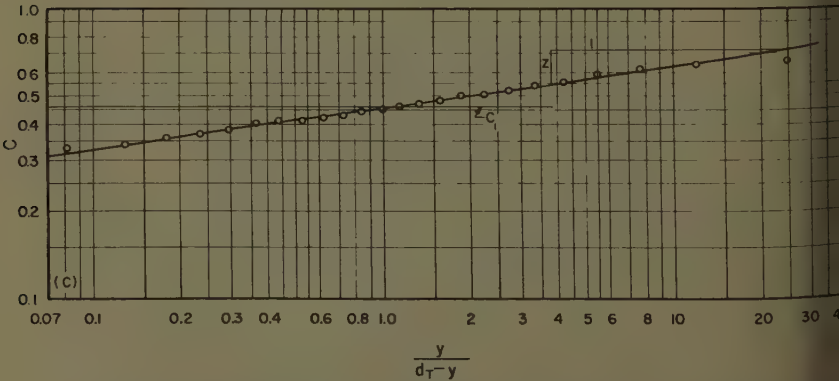


Fig. 7 - Determination of Air-Concentration Distribution Parameters; (a) Definition of Parameters; (b) Parameters in Region Above d_T ; and (c) Parameters in Region Below d_T

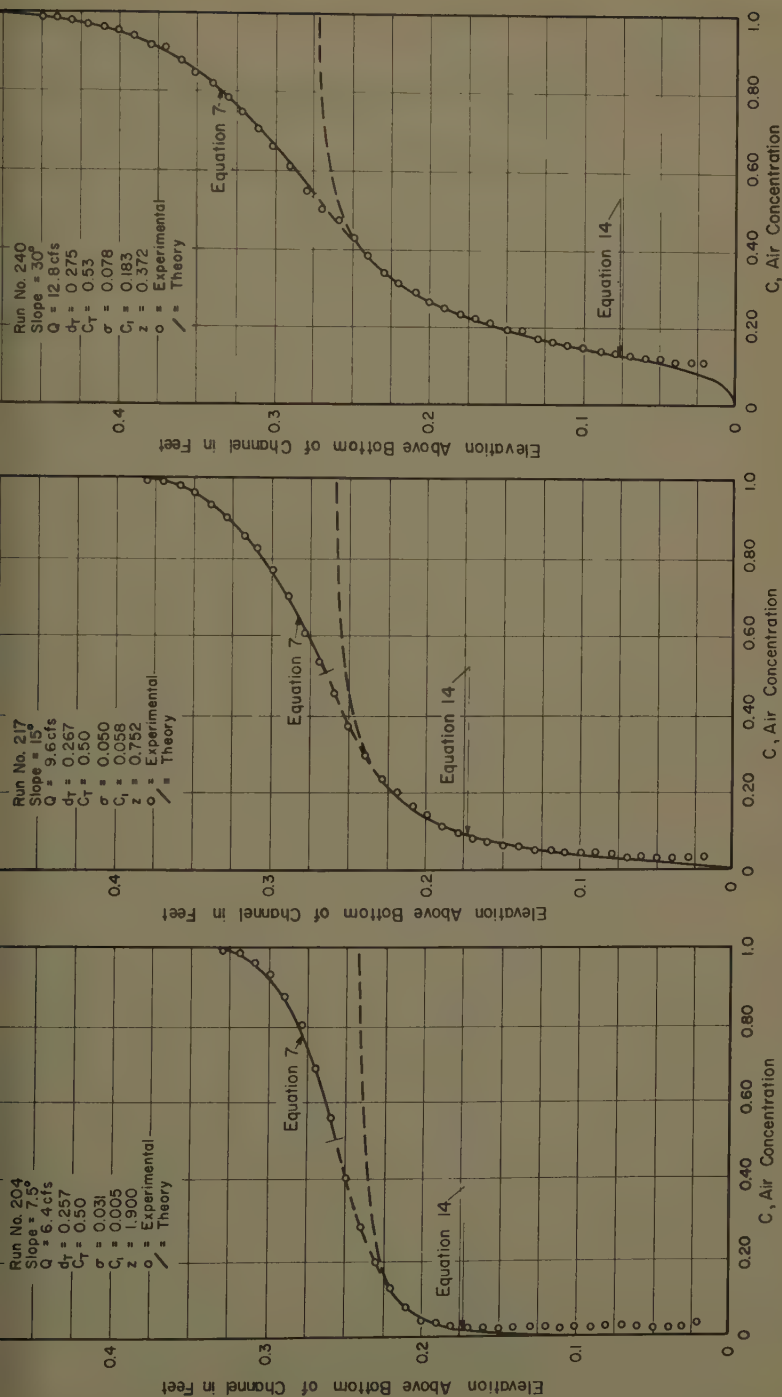
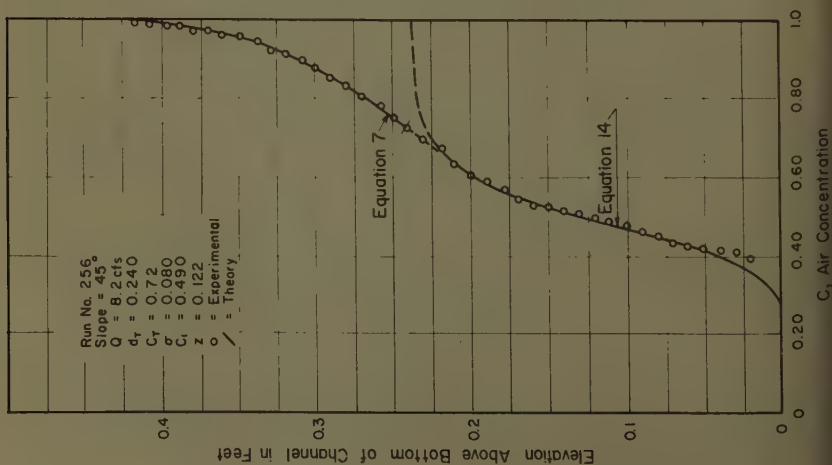
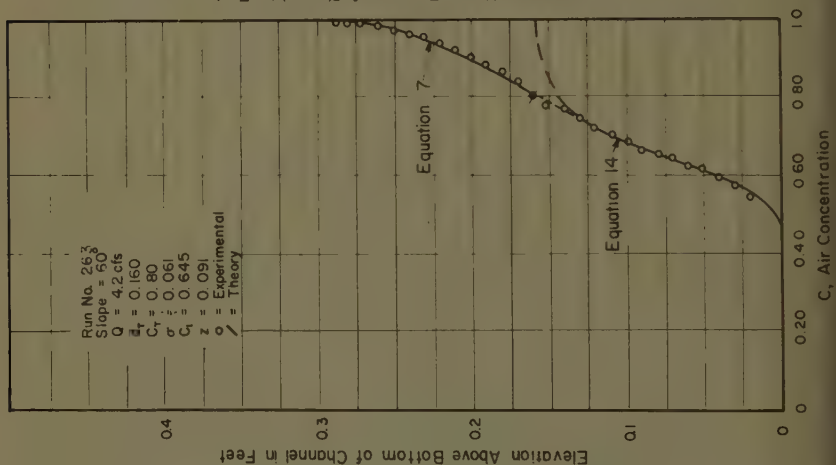
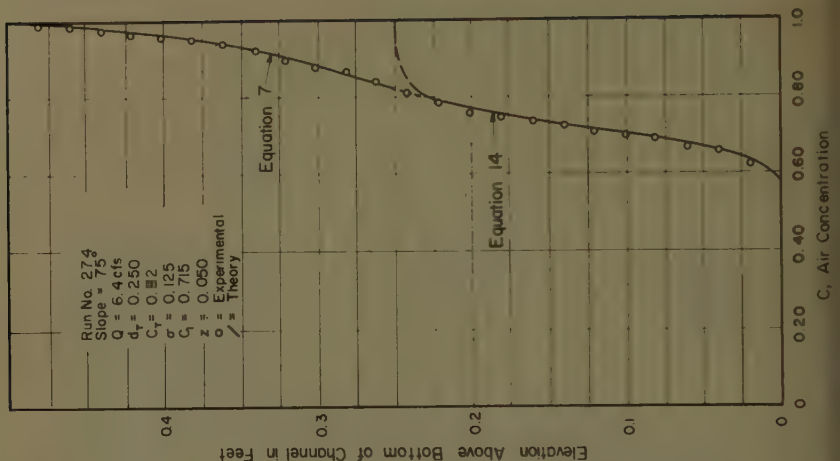


Fig. 8 - Comparison of Measured Concentrations with Theoretical Equations for Slopes of 7.5, 15, and 30 Degrees



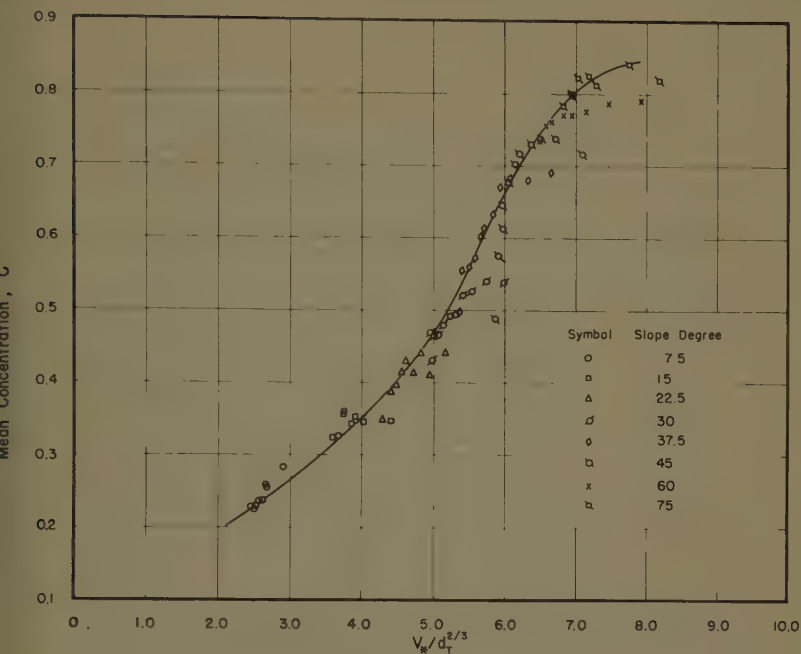


Fig. 10 - Mean Concentration for Entire Flow as a Function of $V_w/d_T^{2/3}$

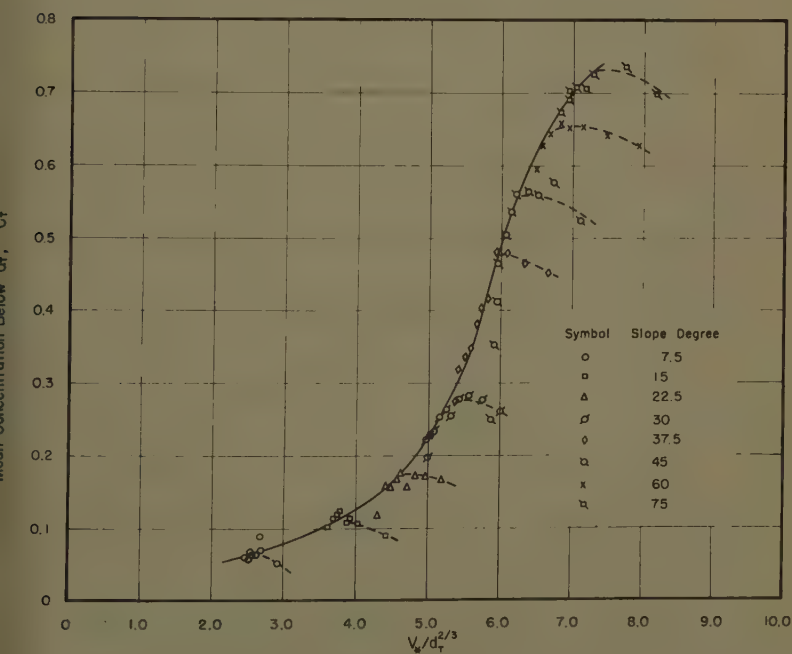


Fig. 11 - Mean Concentration in Region Below Transition Depth as a Function of $V_w/d_T^{2/3}$

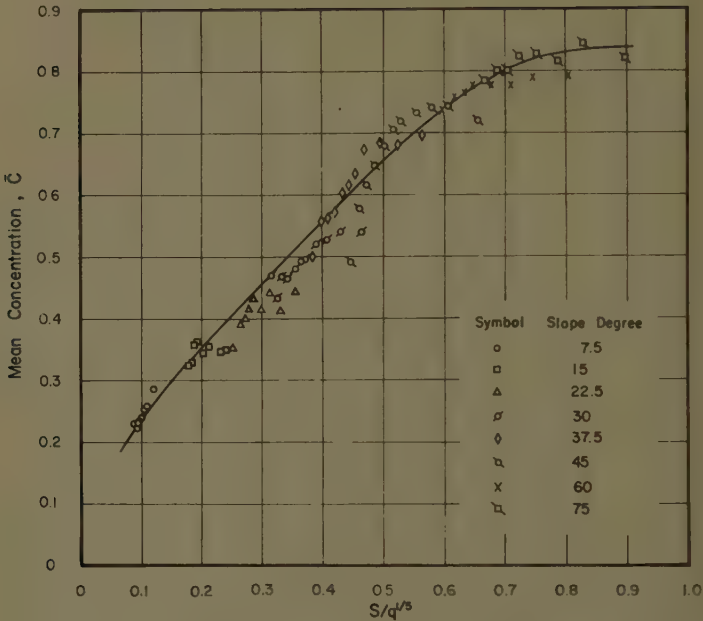


Fig. 12 - Mean Concentration for Entire Flow as a Function of $S/q^{1/5}$

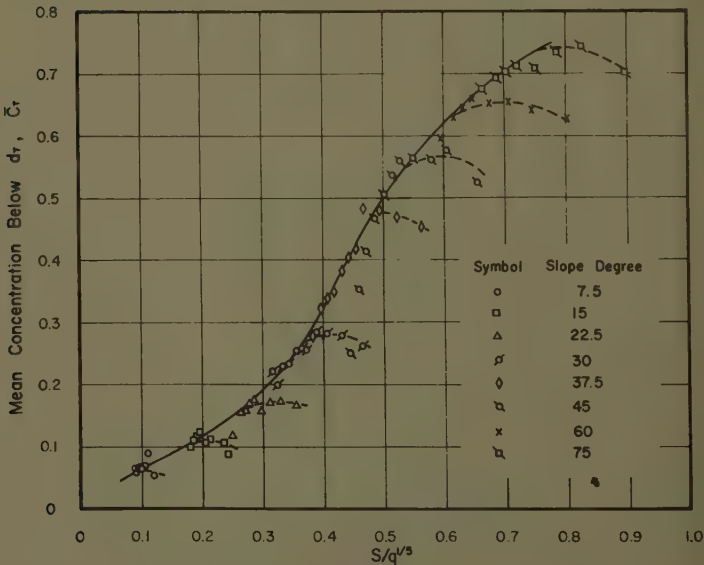


Fig. 13 - Mean Concentration in Region Below Transition Depth as a Function of $S/q^{1/5}$

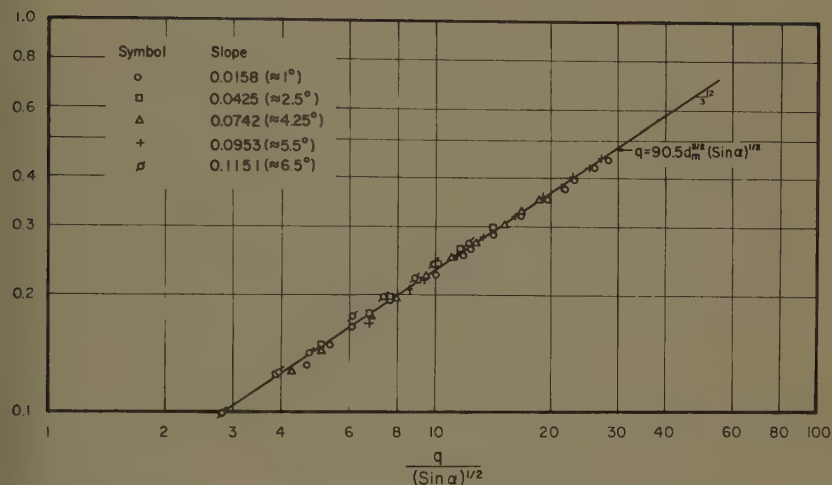


Fig. 14 - Relationship of Depth to Discharge and Slope for Non-aerated Flow in Experimental Channel

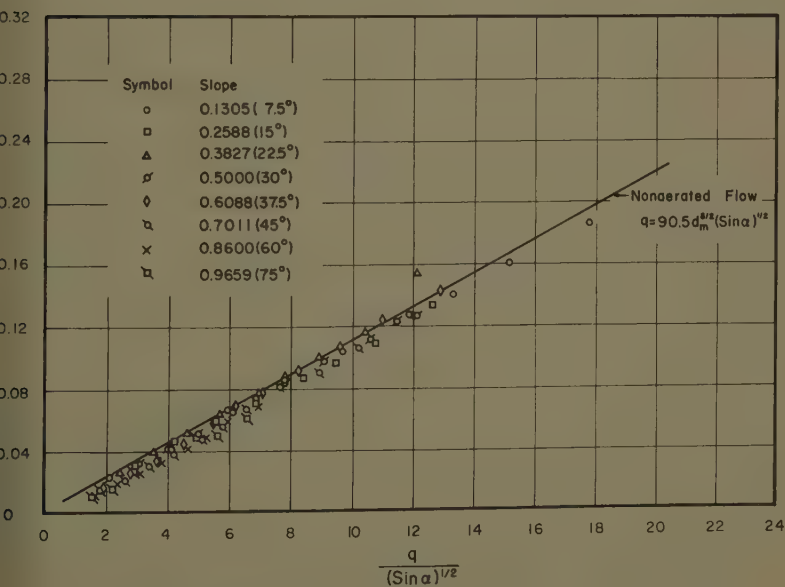


Fig. 15 - Relationship of Depth to Discharge and Slope for Aerated Flow in Experimental Channel

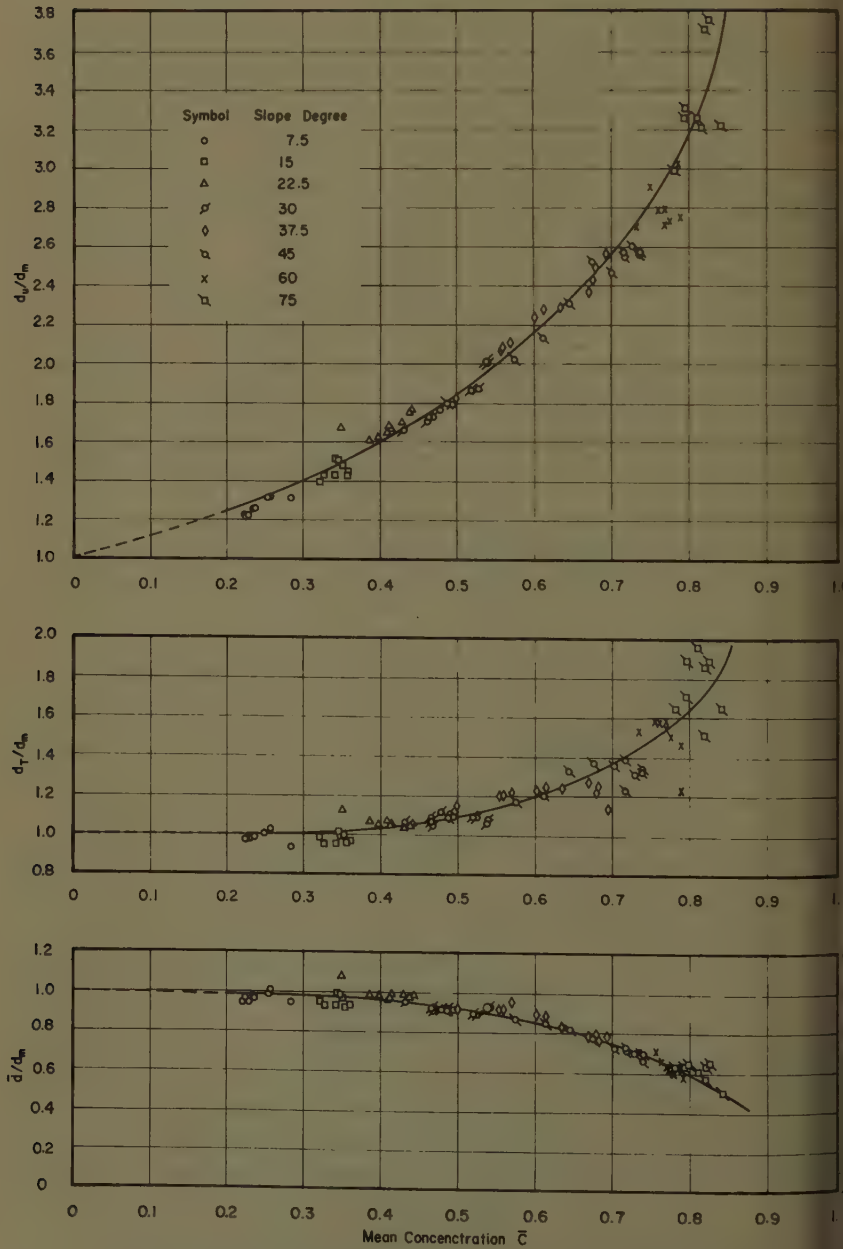


Fig. 16 - The Influence of Air Concentration on Depths of Aerated Flow Relative to Corresponding Nonaerated Flow

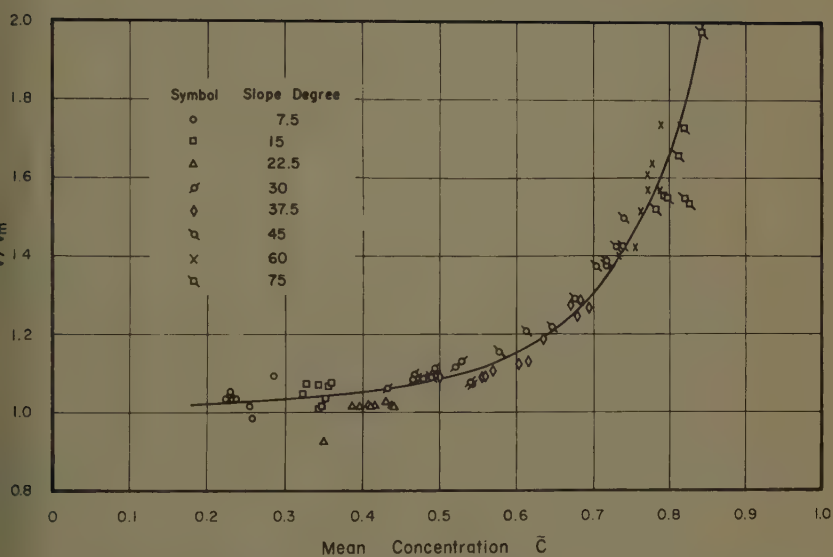


Fig. 17 - The Influence of Air Concentration on Velocity of Aerated Flow Relative to Corresponding Nonaerated Flow

y*	Discharge q in cfs				y* = Distance from channel bed (ft)						
	2.2	3.2	4.2	5.2	6.1	7.2	8.2	9.6	11.2	12.1	12.8
0.02	0.16	0.18	0.17	0.17	0.14	0.15	0.13	0.11	0.11	0.09	0.11
0.03	0.18	0.19	0.17	0.17	0.14	0.15	0.14	0.11	0.11	0.09	0.11
0.04	0.20	0.20	0.18	0.18	0.15	0.16	0.14	0.11	0.11	0.09	0.11
0.05	0.24	0.22	0.20	0.20	0.16	0.17	0.15	0.12	0.12	0.09	0.12
0.06	0.30	0.25	0.21	0.21	0.17	0.17	0.15	0.13	0.12	0.10	0.12
0.07	0.37	0.27	0.24	0.22	0.18	0.19	0.16	0.13	0.13	0.10	0.13
0.08	0.48	0.30	0.26	0.24	0.19	0.20	0.17	0.14	0.13	0.11	0.13
0.09	0.59	0.36	0.30	0.25	0.21	0.21	0.18	0.15	0.14	0.11	0.14
0.10	0.70	0.43	0.34	0.26	0.23	0.22	0.19	0.16	0.15	0.12	0.15
0.11	0.79	0.51	0.40	0.30	0.25	0.23	0.20	0.17	0.16	0.13	0.15
0.12	0.86	0.59	0.46	0.35	0.27	0.25	0.21	0.18	0.17	0.14	0.16
0.13	0.91	0.67	0.54	0.40	0.30	0.27	0.23	0.20	0.18	0.15	0.17
0.14	0.94	0.75	0.61	0.45	0.33	0.29	0.25	0.21	0.18	0.16	0.19
0.15	0.97	0.82	0.69	0.51	0.38	0.33	0.27	0.23	0.20	0.16	0.19
0.16	0.985	0.87	0.75	0.58	0.43	0.37	0.30	0.25	0.21	0.17	0.21
0.17	0.91	0.82	0.66	0.49	0.35	0.31	0.25	0.21	0.17	0.14	0.19
0.18	0.95	0.86	0.71	0.56	0.41	0.35	0.27	0.24	0.19	0.22	0.23
0.19	0.97	0.90	0.79	0.63	0.51	0.46	0.35	0.29	0.23	0.25	0.26
0.20	0.99	0.94	0.83	0.70	0.59	0.54	0.43	0.39	0.31	0.25	0.26
0.21	0.995	0.97	0.87	0.75	0.65	0.55	0.44	0.35	0.28	0.25	0.29
0.22	0.99	0.90	0.80	0.68	0.58	0.48	0.37	0.28	0.21	0.17	0.21
0.23	0.995	0.94	0.85	0.72	0.61	0.51	0.40	0.30	0.21	0.15	0.21
0.24	0.98	0.89	0.82	0.66	0.56	0.46	0.35	0.25	0.17	0.12	0.23
0.25	0.96	0.89	0.81	0.63	0.53	0.43	0.32	0.22	0.14	0.10	0.23
0.26	0.94	0.86	0.78	0.61	0.51	0.41	0.30	0.20	0.12	0.08	0.23
0.27	0.92	0.85	0.77	0.59	0.49	0.39	0.28	0.18	0.10	0.06	0.23
0.28	0.91	0.84	0.76	0.58	0.48	0.38	0.27	0.17	0.09	0.05	0.23
0.29	0.90	0.83	0.75	0.56	0.46	0.36	0.25	0.15	0.08	0.04	0.23
0.30	0.89	0.82	0.74	0.55	0.45	0.35	0.24	0.14	0.07	0.03	0.23
0.31	0.88	0.81	0.73	0.54	0.44	0.34	0.23	0.13	0.06	0.02	0.23
0.32	0.87	0.79	0.71	0.52	0.42	0.32	0.21	0.11	0.05	0.01	0.23
0.33	0.86	0.77	0.69	0.50	0.40	0.30	0.19	0.09	0.04	0.00	0.23
0.34	0.85	0.76	0.68	0.49	0.39	0.29	0.18	0.08	0.03	0.00	0.23
0.35	0.84	0.75	0.67	0.48	0.38	0.28	0.17	0.07	0.02	0.00	0.23
0.36	0.83	0.74	0.66	0.47	0.37	0.27	0.16				

Table I (Continued)

y*	Discharge Q in cfs					60-DEGREE SLOPE				
	2.2	3.2	4.2	5.2	6.4	7.2	8.2	9.6		
0.02	0.51	0.53	0.54	0.55	0.54	0.52	0.50	0.47		
0.03	0.50	0.56	0.57	0.55	0.57	0.54	0.51	0.49		
0.04	0.61	0.59	0.59	0.57	0.58	0.55	0.53	0.50		
0.05	0.65	0.61	0.61	0.59	0.59	0.56	0.54	0.51		
0.06	0.68	0.63	0.62	0.60	0.60	0.58	0.55	0.52		
0.07	0.72	0.65	0.64	0.62	0.62	0.59	0.56	0.53		
0.08	0.76	0.67	0.65	0.63	0.63	0.60	0.57	0.54		
0.09	0.81	0.69	0.66	0.64	0.64	0.61	0.58	0.55		
0.10	0.84	0.72	0.68	0.65	0.65	0.62	0.59	0.56		
0.11	0.87	0.75	0.70	0.66	0.66	0.63	0.59	0.56		
0.12	0.90	0.78	0.72	0.68	0.67	0.64	0.60	0.57		
0.13	0.92	0.81	0.74	0.70	0.68	0.65	0.61	0.58		
0.14	0.94	0.84	0.76	0.72	0.69	0.66	0.62	0.58		
0.15	0.96	0.87	0.78	0.74	0.70	0.67	0.63	0.59		
0.16	0.97	0.89	0.80	0.76	0.71	0.68	0.64	0.60		
0.17	0.98	0.91	0.83	0.78	0.72	0.69	0.65	0.61		
0.18	0.98	0.93	0.86	0.80	0.73	0.70	0.66	0.62		
0.19	0.985	0.94	0.88	0.82	0.75	0.72	0.67	0.63		
0.20	0.99	0.90	0.84	0.77	0.71	0.68	0.64	0.60		
0.21	0.96	0.92	0.86	0.79	0.76	0.70	0.66	0.62		
0.22	0.97	0.93	0.88	0.81	0.77	0.72	0.67	0.63		
0.23	0.98	0.95	0.90	0.83	0.79	0.73	0.68	0.64		
0.24	0.99	0.96	0.91	0.84	0.80	0.74	0.70	0.66		
0.25	0.995	0.97	0.93	0.85	0.82	0.76	0.72	0.68		
0.26	0.98	0.94	0.88	0.81	0.78	0.74	0.70	0.66		
0.27	0.98	0.95	0.89	0.82	0.78	0.74	0.70	0.66		
0.28	0.99	0.96	0.90	0.83	0.79	0.74	0.70	0.66		
0.29	0.995	0.97	0.93	0.85	0.82	0.76	0.72	0.68		
0.30	0.98	0.94	0.88	0.81	0.77	0.72	0.68	0.64		
0.31	0.99	0.96	0.91	0.84	0.80	0.74	0.70	0.66		
0.32	0.99	0.97	0.92	0.85	0.81	0.75	0.71	0.67		
0.33	0.98	0.95	0.90	0.83	0.79	0.74	0.70	0.66		
0.34	0.99	0.96	0.91	0.84	0.80	0.74	0.70	0.66		
0.35	0.995	0.97	0.93	0.85	0.82	0.76	0.72	0.68		
0.36	0.98	0.94	0.88	0.81	0.77	0.72	0.68	0.64		
0.37	0.99	0.96	0.91	0.84	0.80	0.74	0.70	0.66		
0.38	0.995	0.97	0.93	0.85	0.82	0.76	0.72	0.68		
0.39	0.98	0.94	0.88	0.81	0.77	0.72	0.68	0.64		
0.40	0.99	0.96	0.91	0.84	0.80	0.74	0.70	0.66		
0.41	0.99	0.97	0.92	0.85	0.81	0.75	0.71	0.67		
0.42	0.995	0.97	0.93	0.85	0.82	0.76	0.72	0.68		
0.43	0.98	0.94	0.88	0.81	0.77	0.72	0.68	0.64		
0.44	0.99	0.96	0.91	0.84	0.80	0.74	0.70	0.66		
0.45	0.995	0.97	0.93	0.85	0.82	0.76	0.72	0.68		
0.46	0.98	0.94	0.88	0.81	0.77	0.72	0.68	0.64		
0.47	0.99	0.96	0.91	0.84	0.80	0.74	0.70	0.66		

y* = Distance from channel bed (ft.)

y*	Discharge Q in cfs					37.5-DEGREE SLOPE				
	2.2	3.2	4.2	5.2	6.4	7.2	8.2	9.6	11.2	12.8
0.02	0.36	0.36	0.37	0.36	0.29	0.29	0.25	0.19	0.16	0.14
0.03	0.39	0.38	0.40	0.38	0.30	0.30	0.27	0.20	0.17	0.14
0.04	0.41	0.41	0.40	0.38	0.31	0.31	0.28	0.21	0.19	0.15
0.05	0.46	0.43	0.42	0.41	0.32	0.32	0.29	0.23	0.20	0.15
0.06	0.50	0.45	0.44	0.43	0.34	0.34	0.30	0.24	0.21	0.15
0.07	0.55	0.48	0.46	0.45	0.35	0.35	0.31	0.25	0.22	0.17
0.08	0.60	0.50	0.48	0.46	0.37	0.36	0.32	0.25	0.23	0.17
0.09	0.67	0.54	0.50	0.47	0.38	0.37	0.33	0.26	0.23	0.18
0.10	0.73	0.58	0.52	0.49	0.41	0.38	0.34	0.28	0.24	0.19
0.11	0.79	0.62	0.54	0.51	0.42	0.40	0.35	0.30	0.25	0.20
0.12	0.83	0.67	0.57	0.53	0.43	0.41	0.37	0.31	0.26	0.21
0.13	0.87	0.72	0.60	0.58	0.45	0.42	0.39	0.33	0.27	0.22
0.14	0.91	0.77	0.64	0.58	0.47	0.43	0.40	0.34	0.28	0.23
0.15	0.93	0.81	0.69	0.60	0.50	0.45	0.42	0.36	0.30	0.25
0.16	0.96	0.84	0.73	0.63	0.54	0.46	0.43	0.38	0.34	0.29
0.17	0.98	0.87	0.77	0.67	0.57	0.48	0.45	0.40	0.35	0.31
0.18	0.98	0.90	0.81	0.71	0.60	0.52	0.47	0.41	0.36	0.32
0.19	0.99	0.93	0.84	0.74	0.65	0.55	0.50	0.43	0.37	0.33
0.20	0.995	0.95	0.87	0.77	0.70	0.58	0.53	0.45	0.39	0.35
0.21	0.97	0.90	0.81	0.71	0.61	0.56	0.51	0.43	0.38	0.30
0.22	0.98	0.92	0.84	0.74	0.66	0.60	0.55	0.45	0.40	0.32
0.23	0.98	0.94	0.86	0.76	0.68	0.64	0.58	0.48	0.42	0.34
0.24	0.99	0.95	0.89	0.80	0.72	0.68	0.62	0.50	0.45	0.36
0.25	0.97	0.91	0.86	0.76	0.72	0.64	0.59	0.47	0.41	0.38
0.26	0.98	0.93	0.88	0.75	0.75	0.68	0.61	0.51	0.45	0.40
0.27	0.99	0.95	0.90	0.82	0.81	0.71	0.65	0.53	0.46	0.43
0.28	0.995	0.96	0.92	0.85	0.83	0.75	0.65	0.55	0.48	0.46
0.29	0.97	0.94	0.87	0.84	0.73	0.68	0.60	0.49	0.43	0.40
0.30	0.98	0.95	0.90	0.87	0.81	0.73	0.65	0.56	0.49	0.46
0.31	0.99	0.96	0.92	0.89	0.81	0.76	0.68	0.59	0.51	0.48
0.32	0.99	0.97	0.94	0.91	0.86	0.79	0.71	0.64	0.56	0.51
0.33	0.98	0.95	0.93	0.90	0.83	0.77	0.71	0.68	0.61	0.56
0.34	0.99	0.96	0.94	0.91	0.86	0.80	0.75	0.71	0.65	0.60
0.35	0.995	0.97	0.95	0.92	0.88	0.82	0.78	0.74	0.68	0.64
0.36	0.99	0.97	0.95	0.92	0.88	0.82	0.78	0.74	0.68	0.64
0.37	0.995	0.97	0.95	0.92	0.88	0.82	0.78	0.74	0.68	0.64
0.38	0.98	0.95	0.93	0.90	0.86	0.80	0.76	0.71	0.65	0.61
0.39	0.99	0.96	0.94	0.91	0.86	0.80	0.76	0.71	0.65	0.61
0.40	0.99	0.97	0.95	0.92	0.88	0.82	0.78	0.74	0.68	0.64
0.41	0.995	0.97	0.95	0.92	0.88	0.82	0.78	0.74	0.68	0.64
0.42	0.98	0.95	0.93	0.90	0.86	0.80	0.76	0.71	0.65	0.61
0.43	0.99	0.96	0.94	0.91	0.86	0.80	0.76	0.71	0.65	0.61
0.44	0.995	0.97	0.95	0.92	0.88	0.82	0.78	0.74	0.68	0.64
0.45	0.98	0.95	0.93	0.90	0.86	0.80	0.76	0.71	0.65	0.61
0.46	0.99	0.96	0.94	0.91	0.86	0.80	0.76	0.71	0.65	0.61
0.47	0.995	0.97	0.95	0.92	0.88	0.82	0.78	0.74	0.68	0.64

y* = Distance from channel bed (ft.)

Table I (Continued)

y*	Discharge Q in cfs					45-DEGREE SLOPE					75-DEGREE SLOPE								
	2.2	3.2	4.2	5.2	6.2	7.2	8.2	9.6	11.2	12.8	15.0	2.2	3.2	4.2	5.2	6.2	7.2	8.2	9.6
0.02	0.13	0.18	0.22	0.26	0.30	0.34	0.40	0.46	0.52	0.58	0.64	0.02	0.61	0.64	0.67	0.70	0.73	0.76	0.79
0.03	0.16	0.20	0.24	0.28	0.32	0.36	0.42	0.48	0.54	0.60	0.66	0.03	0.64	0.67	0.69	0.71	0.73	0.75	0.77
0.04	0.20	0.24	0.28	0.32	0.36	0.40	0.46	0.52	0.58	0.64	0.70	0.04	0.67	0.70	0.72	0.74	0.76	0.78	0.80
0.05	0.24	0.28	0.32	0.36	0.40	0.44	0.50	0.56	0.62	0.68	0.74	0.05	0.69	0.72	0.74	0.76	0.78	0.80	0.82
0.06	0.28	0.32	0.36	0.40	0.44	0.48	0.54	0.60	0.66	0.72	0.78	0.06	0.72	0.74	0.76	0.78	0.80	0.82	0.84
0.07	0.32	0.36	0.40	0.44	0.48	0.52	0.58	0.64	0.70	0.76	0.82	0.07	0.75	0.77	0.79	0.81	0.83	0.85	0.87
0.08	0.36	0.40	0.44	0.48	0.52	0.56	0.62	0.68	0.74	0.80	0.86	0.08	0.77	0.79	0.81	0.83	0.85	0.87	0.89
0.09	0.40	0.44	0.48	0.52	0.56	0.60	0.66	0.72	0.78	0.84	0.90	0.09	0.80	0.82	0.84	0.86	0.88	0.90	0.92
0.10	0.44	0.48	0.52	0.56	0.60	0.64	0.70	0.76	0.82	0.88	0.94	0.10	0.83	0.85	0.87	0.89	0.91	0.93	0.95
0.11	0.48	0.52	0.56	0.60	0.64	0.68	0.74	0.80	0.86	0.92	0.98	0.11	0.85	0.87	0.89	0.91	0.93	0.95	0.97
0.12	0.52	0.56	0.60	0.64	0.68	0.72	0.78	0.84	0.90	0.96	1.02	0.12	0.87	0.89	0.91	0.93	0.95	0.97	0.99
0.13	0.56	0.60	0.64	0.68	0.72	0.76	0.82	0.88	0.94	1.00	1.06	0.13	0.89	0.91	0.93	0.95	0.97	0.99	1.01
0.14	0.60	0.64	0.68	0.72	0.76	0.80	0.86	0.92	0.98	1.04	1.10	0.14	0.92	0.94	0.96	0.98	1.00	1.02	1.04
0.15	0.64	0.68	0.72	0.76	0.80	0.84	0.90	0.96	1.02	1.08	1.14	0.15	0.94	0.96	0.98	1.00	1.02	1.04	1.06
0.16	0.68	0.72	0.76	0.80	0.84	0.88	0.94	1.00	1.06	1.12	1.18	0.16	0.95	0.97	0.99	1.01	1.03	1.05	1.07
0.17	0.72	0.76	0.80	0.84	0.88	0.92	0.98	1.04	1.10	1.16	1.22	0.17	0.96	0.98	1.00	1.02	1.04	1.06	1.08
0.18	0.76	0.80	0.84	0.88	0.92	0.96	1.02	1.08	1.14	1.20	1.26	0.18	0.97	0.99	1.01	1.03	1.05	1.07	1.09
0.19	0.80	0.84	0.88	0.92	0.96	1.00	1.06	1.12	1.18	1.24	1.30	0.19	0.98	1.00	1.02	1.04	1.06	1.08	1.10
0.20	0.84	0.88	0.92	0.96	1.00	1.04	1.10	1.16	1.22	1.28	1.34	0.20	0.98	1.00	1.02	1.04	1.06	1.08	1.10
0.21	0.88	0.92	0.96	1.00	1.04	1.08	1.14	1.20	1.26	1.32	1.38	0.21	0.98	1.00	1.02	1.04	1.06	1.08	1.10
0.22	0.92	0.96	1.00	1.04	1.08	1.12	1.18	1.24	1.30	1.36	1.42	0.22	0.99	1.01	1.03	1.05	1.07	1.09	1.11
0.23	0.96	1.00	1.04	1.08	1.12	1.16	1.22	1.28	1.34	1.40	1.46	0.23	0.99	1.01	1.03	1.05	1.07	1.09	1.11
0.24	1.00	1.04	1.08	1.12	1.16	1.20	1.26	1.32	1.38	1.44	1.50	0.24	0.99	1.01	1.03	1.05	1.07	1.09	1.11
0.25	1.04	1.08	1.12	1.16	1.20	1.24	1.30	1.36	1.42	1.48	1.54	0.25	0.99	1.01	1.03	1.05	1.07	1.09	1.11
0.26	1.08	1.12	1.16	1.20	1.24	1.28	1.34	1.40	1.46	1.52	1.58	0.26	0.99	1.01	1.03	1.05	1.07	1.09	1.11
0.27	1.12	1.16	1.20	1.24	1.28	1.32	1.38	1.44	1.50	1.56	1.62	0.27	0.99	1.01	1.03	1.05	1.07	1.09	1.11
0.28	1.16	1.20	1.24	1.28	1.32	1.36	1.42	1.48	1.54	1.60	1.66	0.28	0.99	1.01	1.03	1.05	1.07	1.09	1.11
0.29	1.20	1.24	1.28	1.32	1.36	1.40	1.46	1.52	1.58	1.64	1.70	0.29	0.99	1.01	1.03	1.05	1.07	1.09	1.11
0.30	1.24	1.28	1.32	1.36	1.40	1.44	1.50	1.56	1.62	1.68	1.74	0.30	0.99	1.01	1.03	1.05	1.07	1.09	1.11
0.31	1.28	1.32	1.36	1.40	1.44	1.48	1.54	1.60	1.66	1.72	1.78	0.31	0.99	1.01	1.03	1.05	1.07	1.09	1.11
0.32	1.32	1.36	1.40	1.44	1.48	1.52	1.58	1.64	1.70	1.76	1.82	0.32	0.99	1.01	1.03	1.05	1.07	1.09	1.11
0.33	1.36	1.40	1.44	1.48	1.52	1.56	1.62	1.68	1.74	1.80	1.86	0.33	0.99	1.01	1.03	1.05	1.07	1.09	1.11
0.34	1.40	1.44	1.48	1.52	1.56	1.60	1.66	1.72	1.78	1.84	1.90	0.34	0.99	1.01	1.03	1.05	1.07	1.09	1.11
0.35	1.44	1.48	1.52	1.56	1.60	1.64	1.70	1.76	1.82	1.88	1.94	0.35	0.99	1.01	1.03	1.05	1.07	1.09	1.11
0.36	1.48	1.52	1.56	1.60	1.64	1.68	1.74	1.80	1.86	1.92	1.98	0.36	0.99	1.01	1.03	1.05	1.07	1.09	1.11
0.37	1.52	1.56	1.60	1.64	1.68	1.72	1.78	1.84	1.90	1.96	2.02	0.37	0.99	1.01	1.03	1.05	1.07	1.09	1.11
0.38	1.56	1.60	1.64	1.68	1.72	1.76	1.82	1.88	1.94	2.00	2.06	0.38	0.99	1.01	1.03	1.05	1.07	1.09	1.11
0.39	1.60	1.64	1.68	1.72	1.76	1.80	1.86	1.92	1.98	2.04	2.10	0.39	0.99	1.01	1.03	1.05	1.07	1.09	1.11
0.40	1.64	1.68	1.72	1.76	1.80	1.84	1.90	1.96	2.02	2.08	2.14	0.40	0.99	1.01	1.03	1.05	1.07	1.09	1.11
0.41	1.68	1.72	1.76	1.80	1.84	1.88	1.94	2.00	2.06	2.12	2.18	0.41	0.99	1.01	1.03	1.05	1.07	1.09	1.11
0.42	1.72	1.76	1.80	1.84	1.88	1.92	1.98	2.04	2.10	2.16	2.22	0.42	0.99	1.01	1.03	1.05	1.07	1.09	1.11
0.43	1.76	1.80	1.84	1.88	1.92	1.96	2.02	2.08	2.14	2.20	2.26	0.43	0.99	1.01	1.03	1.05	1.07	1.09	1.11
0.44	1.80	1.84	1.88	1.92	1.96	2.00	2.06	2.12	2.18	2.24	2.30	0.44	0.99	1.01	1.03	1.05	1.07	1.09	1.11
0.45	1.84	1.88	1.92	1.96	2.00	2.04	2.10	2.16	2.22	2.28	2.34	0.45	0.99	1.01	1.03	1.05	1.07	1.09	1.11
0.46	1.88	1.92	1.96	2.00	2.04	2.08	2.14	2.20	2.26	2.32	2.38	0.46	0.99	1.01	1.03	1.05	1.07	1.09	1.11
0.47	1.92	1.96	2.00	2.04	2.08	2.12	2.18	2.24	2.30	2.36	2.42	0.47	0.99	1.01	1.03	1.05	1.07	1.09	1.11
0.48	1.96	2.00	2.04	2.08	2.12	2.16	2.22	2.28	2.34	2.40	2.46	0.48	0.99	1.01	1.03	1.05	1.07	1.09	1.11
0.49	2.00	2.04	2.08	2.12	2.16	2.20	2.26	2.32	2.38	2.44	2.50	0.49	0.99	1.01	1.03	1.05	1.07	1.09	1.11

ys = Distance from channel bed (ft)

y* = Distance from channel bed (ft)

y* = Distance from channel bed (ft)

APPENDIX C

(Table II - Summary of Experimental Measurements—Rough Channel)

Run	Slope	Temp.	Disch.	\bar{d}	j_u	d_T	$\bar{d}d_T^{1/2}$	$q/S^{1/2}$	
200	7.5°	22.3	2.2	0.1209	0.169	0.120	0.0418	4.06	0.2
201		0.4	3.2	0.1642	0.215	0.166	0.0669	5.90	0.2
202		0	4.2	0.1937	0.260	0.197	0.0860	7.75	0.2
203		0	5.2	0.2204	0.289	0.224	0.1043	9.61	0.2
204		0	6.4	0.2515	0.329	0.257	0.1274	11.80	0.2
205		0	7.2	0.2671	0.347	0.275	0.1400	13.29	0.2
206		0	8.2	0.2943	0.380	0.298	0.1605	15.10	0.2
207		0.4	9.6	0.3247	0.421	0.330	0.1865	17.71	0.2
210	15°	21.0	2.2	0.1010	0.115	0.102	0.0322	2.88	0.2
211		0	3.2	0.1289	0.197	0.132	0.0468	4.18	0.2
212		0	4.2	0.1514	0.234	0.157	0.0630	5.50	0.2
213		0	5.2	0.1701	0.260	0.174	0.0710	6.82	0.2
214		0	6.4	0.1937	0.303	0.200	0.0866	8.37	0.2
215		0	7.2	0.2087	0.323	0.215	0.0968	9.43	0.2
216		0	8.2	0.2275	0.338	0.232	0.1097	10.73	0.2
217		0	9.6	0.2591	0.383	0.267	0.1338	12.57	0.2
220	22.5°	19.6	2.2	0.0866	0.159	0.095	0.0273	2.37	0.2
221		0.8	3.2	0.1130	0.192	0.124	0.0396	3.45	0.2
222		0	4.2	0.1358	0.243	0.145	0.0517	4.53	0.2
223		0.1	5.2	0.1572	0.268	0.166	0.0640	5.62	0.2
224		0	6.4	0.1763	0.310	0.190	0.0768	6.90	0.2
225		0.1	7.2	0.1923	0.329	0.208	0.0877	7.77	0.2
226		0.1	8.2	0.2116	0.351	0.228	0.1009	8.85	0.2
227		0.8	9.6	0.2329	0.380	0.253	0.1170	10.36	0.2
228	30.0°	1.2	12.8	0.2855	0.440	0.296	0.1554	12.08	0.2
230		21.0	2.2	0.0760	0.165	0.087	0.0224	2.07	0.2
231		1.2	3.2	0.0980	0.213	0.115	0.0332	3.01	0.2
232		0	4.2	0.1125	0.238	0.139	0.0419	3.96	0.2
233		0	5.2	0.1307	0.273	0.160	0.0522	4.91	0.2
234		1.2	6.4	0.1530	0.303	0.183	0.0655	6.03	0.2
235		0.2	7.2	0.1644	0.325	0.201	0.0736	6.80	0.2
236		0.2	8.2	0.1809	0.348	0.220	0.0848	7.72	0.2
237		1.0	9.6	0.2008	0.376	0.238	0.0980	9.35	0.2
238		0.2	11.2	0.2202	0.413	0.260	0.1121	10.55	0.2
239		0.2	12.1	0.2392	0.422	0.270	0.1241	11.41	0.2
240		1.0	12.8	0.2424	0.457	0.275	0.1271	12.05	0.2

Table II - Summary of Experimental Measurements—Rough Channel

C_T	C_f	\bar{V}	V_{*c}	$V_{*c}/d_T^{2/3}$	$Re \times 10^{-5}$	z	σ	\bar{V}/V_m
0.45	0.008	12.13	0.710	2.92	5.65	1.920	0.022	1.059
0.50	0.007	12.97	0.809	2.67	4.52	1.550	0.024	0.986
0.50	0.005	14.45	0.909	2.68	5.91	2.150	0.024	1.017
0.50	0.007	15.75	0.969	2.62	7.16	1.590	0.028	1.033
0.50	0.005	16.95	1.039	2.56	9.05	1.900	0.031	1.034
0.54	0.006	17.97	1.074	2.54	10.23	1.660	0.034	1.054
0.48	0.004	18.55	1.119	2.51	11.46	1.750	0.035	1.036
0.50	0.006	19.71	1.178	2.46	13.60	0.645	0.040	1.046
0.50	0.031	14.50	0.923	4.41	5.58	1.255	0.023	1.018
0.50	0.047	16.53	1.050	4.04	4.53	0.935	0.028	1.014
0.50	0.060	18.50	1.144	3.92	6.03	0.785	0.033	1.036
0.47	0.067	20.40	1.206	3.86	7.34	0.613	0.038	1.071
0.46	0.083	22.0	1.292	3.77	9.14	0.527	0.045	1.073
0.50	0.072	23.0	1.340	3.73	10.23	0.622	0.047	1.072
0.48	0.067	24.0	1.396	3.63	11.59	0.630	0.049	1.074
0.50	0.058	24.7	1.494	3.60	13.65	0.752	0.050	1.047
0.55	0.107	16.55	1.081	5.19	5.71	0.693	0.028	1.015
0.55	0.115	18.85	1.235	4.96	4.98	0.665	0.032	1.024
0.52	0.123	20.6	1.338	4.84	6.21	0.507	0.041	1.015
0.50	0.116	22.1	1.430	4.72	7.58	0.490	0.046	1.014
0.50	0.140	24.1	1.530	4.62	9.54	0.388	0.052	1.028
0.53	0.123	24.9	1.600	4.56	10.75	0.507	0.058	1.020
0.53	0.107	25.8	1.676	4.49	12.20	0.547	0.058	1.014
0.57	0.099	27.5	1.768	4.41	14.77	0.700	0.055	1.018
0.50	0.063	29.9	1.911	4.30	19.10	0.735	0.064	0.923
0.55	0.222	19.30	1.182	6.00	6.33	0.326	0.035	1.078
0.55	0.240	21.7	1.360	5.75	5.42	0.314	0.041	1.077
0.61	0.245	24.9	1.494	5.55	7.18	0.345	0.041	1.029
0.58	0.242	26.5	1.605	5.43	8.79	0.306	0.049	1.113
0.58	0.213	27.9	1.715	5.31	11.04	0.366	0.052	1.094
0.60	0.227	29.2	1.800	5.25	12.23	0.340	0.049	1.102
0.61	0.200	30.2	1.880	5.16	13.83	0.420	0.058	1.086
0.60	0.186	31.9	1.958	5.09	16.30	0.420	0.061	1.085
0.60	0.185	33.9	2.045	5.02	18.36	0.431	0.068	1.094
0.57	0.157	33.8	2.085	5.00	18.98	0.429	0.069	1.060
0.53	0.183	35.2	2.105	4.96	20.80	0.372	0.078	1.086

Table II (Continued)

Run	Slope	Temp.	Disch.	\bar{u}	d_u	d_T	$\bar{d}d_T^{1/2}$	$q/s^{1/2}$	\bar{C}
240 $\frac{1}{2}$	37.5°	19.6	2.2	0.0605	0.198	0.085	0.0176	1.88	0.69
241		16.8	3.2	0.0783	0.245	0.120	0.0271	2.73	0.64
242		16.8	4.2	0.0923	0.291	0.148	0.0355	3.59	0.61
243		16.8	5.2	0.1073	0.326	0.175	0.0449	4.45	0.60
244		5.0	6.4	0.1317	0.361	0.195	0.0582	5.46	0.59
245		10.6	7.2	0.1494	0.388	0.212	0.0688	6.15	0.62
246		9.3	8.2	0.1638	0.413	0.227	0.0780	7.01	0.60
247		10.5	9.6	0.1855	0.433	0.250	0.0927	8.21	0.59
248		10.3	11.2	0.2064	0.471	0.272	0.1075	9.57	0.58
249		10.3	12.8	0.2275	0.514	0.300	0.1246	10.93	0.59
250		10.3	15.0	0.2521	0.505	0.315	0.1415	12.81	0.58
250 $\frac{1}{2}$	45°	18.6	2.2	0.0530	0.188	0.090	0.0159	1.74	0.71
251		12.9	3.2	0.0625	0.240	0.125	0.0221	2.53	0.70
252		12.8	4.2	0.0791	0.303	0.151	0.0307	3.33	0.70
253		12.8	5.2	0.0921	0.342	0.172	0.0382	4.13	0.70
254		12.9	6.4	0.1065	0.378	0.205	0.0482	5.07	0.70
255		12.0	7.2	0.1182	0.400	0.220	0.0555	5.71	0.70
256		12.1	8.2	0.1361	0.422	0.240	0.0667	6.50	0.69
257		11.9	9.6	0.1500	0.452	0.260	0.0815	7.61	0.69
258		18.5	11.2	0.1782	0.462	0.260	0.0910	8.87	0.69
259		18.5	12.8	0.2029	0.479	0.275	0.1063	10.14	0.69
260		19.8	15.0	0.2397	0.469	0.278	0.1280	11.90	0.68
261	60°	19.8	2.2	0.0397	0.190	0.085	0.0116	1.58	0.77
262		14.5	3.2	0.0540	0.260	0.126	0.0195	2.29	0.77
263		18.0	4.2	0.0648	0.290	0.160	0.0259	3.01	0.77
264		18.6	5.2	0.0759	0.331	0.190	0.0330	3.73	0.77
265		18.6	6.4	0.0887	0.389	0.220	0.0416	4.59	0.77
266		19.8	7.2	0.1003	0.423	0.240	0.0492	5.16	0.77
267		19.2	8.2	0.1163	0.476	0.260	0.0593	5.88	0.77
268		14.5	9.6	0.1299	0.491	0.280	0.0687	6.88	0.77
270	75°	19.8	2.2	0.0382	0.212	0.100	0.0121	1.49	0.81
271		22.0	3.2	0.0429	0.273	0.140	0.0161	2.17	0.81
272		22.0	4.2	0.0618	0.333	0.200	0.0275	2.85	0.81
273		21.3	5.2	0.0764	0.440	0.220	0.0358	3.53	0.81
274		21.3	6.4	0.0874	0.501	0.250	0.0457	4.35	0.81
275		20.9	7.2	0.0936	0.465	0.275	0.0490	4.88	0.79
276		20.9	8.2	0.1016	0.500	0.270	0.0328	5.56	0.79
277		20.9	9.6	0.1124	0.520	0.290	0.0606	6.51	0.79

Table II (Continued)

	C_T	C_L	\bar{V}	V_*	$V_*/d_T^{2/3}$	$Re \times 10^{-5}$	z	σ	\bar{V}/V_m
	0.63	0.431	24.2	1.292	6.66	7.49	0.164	0.048	1.270
	0.67	0.450	27.2	1.538	6.33	11.10	0.152	0.056	1.248
	0.68	0.462	30.3	1.706	6.09	15.23	0.142	0.061	1.287
	0.69	0.472	32.3	1.857	5.94	19.13	0.140	0.068	1.277
	0.68	0.402	32.3	1.955	5.82	15.40	0.177	0.073	1.188
	0.62	0.392	32.1	2.04	5.73	19.60	0.158	0.078	1.130
	0.63	0.363	33.4	2.11	5.67	21.0	0.192	0.081	1.125
	0.64	0.317	34.5	2.22	5.59	24.8	0.250	0.080	1.106
	0.62	0.310	36.1	2.31	5.51	28.1	0.237	0.090	1.091
	0.64	0.292	37.5	2.43	5.42	32.1	0.290	0.089	1.090
	0.61	0.242	39.7	2.49	5.38	35.7	0.318	0.080	1.091
	0.71	0.510	27.7	1.430	7.10	8.80	0.140	0.046	1.378
	0.76	0.565	34.1	1.634	6.73	12.60	0.113	0.051	1.502
	0.75	0.550	35.4	1.852	6.52	16.31	0.113	0.068	1.427
	0.73	0.555	37.7	1.977	6.38	19.75	0.087	0.078	1.423
	0.72	0.555	40.0	2.16	6.21	25.3	0.092	0.079	1.389
	0.73	0.525	40.6	2.24	6.15	26.7	0.113	0.082	1.372
	0.72	0.490	40.1	2.34	6.06	29.0	0.122	0.080	1.289
	0.70	0.453	40.0	2.43	5.98	31.0	0.143	0.090	1.218
	0.65	0.398	41.8	2.43	5.98	38.6	0.151	0.088	1.208
	0.64	0.326	42.0	2.50	5.91	41.0	0.234	0.095	1.157
	0.60	0.217	41.7	2.55	5.86	44.0	0.346	0.083	1.092
	0.78	0.613	37.0	1.539	7.93	11.50	0.107	0.053	1.737
	0.80	0.630	38.8	1.873	7.48	15.61	0.102	0.061	1.565
	0.80	0.545	43.2	2.11	7.15	24.1	0.091	0.061	1.636
	0.82	0.645	45.7	2.30	6.95	30.8	0.098	0.073	1.606
	0.81	0.657	48.2	2.49	6.84	37.6	0.0806	0.090	1.570
	0.80	0.640	47.8	2.58	6.68	42.1	0.086	0.095	1.513
	0.78	0.610	47.0	2.69	6.59	44.0	0.087	0.098	1.424
	0.77	0.590	49.3	2.79	6.50	44.2	0.093	0.102	1.401
	0.83	0.690	38.4	1.767	8.18	14.32	0.093	0.060	1.730
	0.87	0.750	49.7	2.09	7.75	26.7	0.089	0.067	1.976
	0.85	0.730	45.4	2.50	7.30	34.6	0.063	0.084	1.654
	0.84	0.700	45.5	2.62	7.18	37.7	0.067	0.100	1.535
	0.82	0.715	48.9	2.79	7.03	46.1	0.050	0.125	1.547
	0.83	0.701	51.3	2.915	6.93	52.3	0.0579	0.094	1.550
	0.81	0.687	53.8	2.90	6.93	54.4	0.0506	0.118	1.555
	0.80	0.670	56.9	3.01	6.84	61.8	0.05075	0.106	1.521

Table II (Continued)

